Genetic Mapping of Candidates of Hereditary Microcephaly Genes

by

Abdul Aziz

Department of Biochemistry
Faculty of Biological Sciences
Quaid-i-Azam University
Islamabad
2008

Genetic Mapping of Candidtes of Hereditary Microcephaly Genes

A thesis submitted in partial fulfillment of the requirements for the degree of

Master of Philosophy in

Biochemistry/ Molecular Biology

by

Abdul Aziz

Department of Biochemistry
Faculty of Biological Sciences
Quaid-i-Azam University
Islamabad
2008

CERTIFICATE

The Department of Biochemistry, Faculty of Biological Sciences, Quaid-i-Azam University Islamabad, accepts this thesis submitted by **Abdul Aziz** in its present form, as satisfying the thesis requirements for the degree of Master of Philosophy in Biochemistry / Molecular Biology.

Internal Examiner: _____
Dr. Wasim Ahmad

External Examiner: _____
Dr. Mahmood Akhtar Kayani

Chairman: _____
Dr. Wasim Ahmad

Dated: 17/03/2008

DECLARATION

I hereby declare that the work presented in the following thesis is my own effort, except where otherwise acknowledged, and that the thesis is my own composition. No part of the thesis has been previously presented for any other degree.

Abdul Aziz

DEDICATED

TO

MY BELOVED PARENTS

ACKNOWLEDGEMENTS

All praises for Almighty 'Allah' The most Merciful, without Allah's divine help, I would not have been able to achieve anything in my life. It is His benevolence and compassion that He opened new avenues and vistas of knowledge to our puny mind and choice us to serve humanity. Peace and blessings be upon the Holy Prophet Hazrat Muhammad (S.A.S), who exhorted his followers to seek knowledge from cradle to grave.

I'm feeling pride to articulate some obsession about my respected teacher and research supervisor, Dr. Wasim Ahmad, Professor and Chairman Department of Biochemistry, Quaid-i-Azam University Islamabad, without whose help this uphill task would have been impossible to achieve. I am truly inspired by him. His energy, optimism, intelligence and continuous encouragement at every step during the course of this whole project enabled me to achieve my goals. He has left an everlasting and perennial mark of his dynamic personality on my heart.

My love and affection to my parents knows no limit. I still feel like a child with his tiny finger held in his parents hands learning how to walk. My father, my ideal, I always wants to be like him, and this had led me to achieve this goal. Words become meaningless when I see them as icons of strength for being what I am today. I owe deep gratitude to my brothers and sister for their unmatched support, love and prayers. I deeply appreciate my whole family who has constantly prayed for me during my whole stay here in the university.

I also want to acknowledge the constant and diligent cooperation and support of my seniors. They profited me as per their experience and made a lot possible for me. Thanks a lot to my all lab fellows, my class fellows who not only contributed in areas of academic and research but also in sphere of friendship, sincerity and amiability.

I am thankful to my friends for their nice and sweet company and for their constructive advices. The good time spent with them can never be erased from my memories.

Abdul Aziz

Table of Contents — Page Numbers

List of Abbreviations

µl	Micro litre
A	Adenine
aa	Aminoacid
Amp	Amplification
ANGPT2	Angiopoietin-2
ASPM	Abnormal spindle like microcephaly associated
bp	Base pairs
BRCA1	Breast cancer gene
BRCT	C-terminal portion of the BRCA-1 gene
BRIT1	BRCT-repeat inhibitor of TERT expression 1
C	Cytosine
C- Terminus	Carboxyl terminus
CAG	Glutamine
CDC45	Cell division cycle 45
CDK1	Cyclin-dependent kinase 1
CDK5	Cyclin-dependent kinase 5
CDK5RAP2	CDK5 regulatory subunit-associated protein 2
cDNA	Complementary DNA
CENPJ	Centromeric protein J
CHK1	DNA damage check point kinase 1
CHLC	Cooperative human linkage centre
cM	Centimorgan
Cnn	Centrosomin
CPAP	Centrosomal protein 4.1-associated protein

DC	Digital camera
Del	Deletion
dNTPs	Deoxy nucleotides triphosphates
E	Embryonic days
EDTA	Ethylene-diamine-tetra-acetic acid
ELISA	Enzyme-linked immuno sorbent assay
EPB41	Erythrocyte membrane protein band 4.1
G	Guanine
G phase	Growth phase
HC	Head circumference
INPP5E	Inositol polyphosphate-5-phosphatase E
Ins	Insertion
IQ	Intelligence quotient
IR	Ionizing irradiation
Kb	Kilo bases
KDa	Kilo dalton
M phase	Mitotic phase
Mb	Mega bases
MCPH	Autosomal recessive primary microcephaly
MIM	Mendelian inheritance in man
ml	Milli litre
mm	Milli molar
MRI	Magnetic resonance imaging
N- Terminus	Amino terminus
NBS1	Nijmegen breakage syndrome 1

NMR	Nuclear magnetic resonance
OD	Optical density
ORF	Open reading frame
PCC	Premature chromosomal condensation
PCR	Polymerase chain reaction
pH	Hydrogen ion concentrations
RNAi	RNA interference
rpm	Revolutions per minute
RT PCR	Reverse transcriptase polymerase chain reaction
S	Serine
S phase	Stationary phase
SD	Standard deviation
SDS	Sodium dodocyl sulphate
Ser	Serine
SiRNA	Small interfering RNA
T	Thymine
T.S.R	Template suppression reagent
Taq	Thermus aquaticus
TBE	Tris borate EDTA
TCP 10	T-complex 10
TE	Tris- EDTA
TEMED	N, N, N', N'- Tetra methyl ethylene diamine
Ter	Terminated
TGG	Tryptophane
UV	Ultra violet

ABSTRACT

Autosomal recessive primary microcephaly (MCPH), a rare neurodevelopmental disorder, is characterized by reduced head circumference of at least 4 standard deviations below the age- and sex- related population specific means; associated with non progressive mental retardation of variable degree but no other neurological deficit. In individuals with MCPH phenotype, the brain weight is markedly reduced and the cerebral cortex is disproportionately small with no major abnormalities in cortical architecture. Primary microcephaly displays genetic heterogeneity with eight loci (MCPH1 to MCPH8) mapped to date. For these five genes *Microcephalin* at MCPH1; *CDK5RAP2* at MCPH3; *ASPM* at MCPH5; *CENPJ* at MCPH6 and *INPP5E* at MCPH7 are discovered so far. Three MCPH proteins ASPM, CDK5RAP2 and CENPJ are centrosomal components and recently have been shown to be localized in the midbodies and hence the observations support a model of neurogenesis in which spindle dynamics and cellular abscission are coordinated.

In the study, presented here, four families (A, B, C and D) suffering from MCPH representing different regions of Pakistan were studied. To elucidate the gene defect in these families, linkage was performed by genotyping polymorphic microsatellite markers linked to seven known primary microcephaly loci. Genotyping analysis showed linkage of three families (A, B and C) to MCPH5 locus harboring *ASPM* gene. Therefore, *ASPM* gene was sequenced in affected and normal individuals of these three families.

In families A and B, the entire coding region and splice junctions of *ASPM* gene were screened in two affected and one normal individual of the families. Sequence analysis failed to detect pathogenic sequence variant suggesting that the mutation is probably present in the regulatory sequences of the gene. Family C, showed a previously characterized mutation (3978 G > A) in exon 17 of the *ASPM* gene.

Genotyping analysis showed linkage of family D to MCPH7 locus harboring *INPP5E* gene. Therefore, *INPP5E* gene was sequenced in two affected and one normal individuals of the family. Sequence analysis of the entire coding region and splice junctions of *INPP5E* gene failed to detect pathogenic sequence variant suggesting that the mutation is probably present in the regulatory sequences of the gene.

INTRODUCTION

INTRODUCTION

The term Microcephaly refers to the clinical finding of head circumference (HC) significantly smaller than expected for a normal individual, taking into consideration age and sex. Autosomal recessive primary microcephaly (MCPH; MIM 251200) is a neuro-developmental disorder. It is characterized by two principal features, microcephaly present at birth and non-progressive mental retardation. The microcephaly is the consequence of a small but architecturally normal brain, and it is the cerebral cortex that shows the greatest size reduction. The importance of the clinical finding of microcephaly – reduced cranial size – is that it is strongly correlated with mental retardation (Dolk *et al.*, 1991). Individuals with an HC of -3 SD and normal intelligence are occasionally reported (Trimborn *et al.*, 2005), but individuals with an HC of -4 SD or less and normal intelligence are very rare (Teebi *et al.*, 1987). The greater the degree of Microcephaly, greater is the risk and severity of mental retardation (Cox *et al.*, 2006).

In humans the cerebral cortex represent a highly developed structure concerned with the most familiar functions we associate with the human brain. It is the highly convoluted external surface of the brain which is approximately 2 mm thick. The cerebral cortex is made up of neuron and supporting cells (glial cells) and functions to correlate information from many sources to maintain cognitive function (all aspects of perceiving, thinking and remembering). Its distinctive shape arose during evolution as the volume of the cortex increased more rapidly than the cranial volume. This differential rate of evolutionary development resulted in the convolution of the surface and the folding of the total structure of the cortex.

At birth, the human brain is approximately three times larger than that of our closest primate relatives. Brain growth occurs both in the pre- and post-natal period (in the first three years of human life, the brain becomes four times bigger than that at birth). The human skull is designed to accommodate this change through growth of skull bones and delayed closure of the sutures between the skull bones.

Types of Microcephaly

Microcephaly is being divided into primary and secondary microcephaly on the basis of onset of this abnormality. The crucial difference between these groupings is that primary microcephaly is usually a static developmental anomaly, whereas secondary microcephaly indicates a progressive neurodegenerative condition (Qazi and Reed, 1973; Opitz and Holt, 1990; Dobyns, 2002; Rosenberg *et al.,* 2002).

Primary Microcephaly

The terms primary microcephaly or 'true microcephaly' are used to describe a subclass of microcephaly, a condition which is genetic in etiology, with many causes having autosomal recessive mode of inheritance in the absence of environmental, metabolic or cytogenetic aetiologies. In 'true microcephaly' the sloping forehead was the defining feature; however, it is not seen in all the cases of primary microcephaly (Bundey, 1997; Dobyns, 2002; Roberts *at el.,* 2002). In affected individuals with Primary microcephaly, the brain fails to grow to the correct size during pregnancy, occurring an abnormally small brain is caused by anomalous development during the first 32 weeks of gestation. Primary microcephaly therefore is likely to be due to a reduced production of neurons. Current studies suggest that primary microcephaly is caused by a decrease in the number of neurons generated during neurogenesis.

Secondary Microcephaly

The number of disorders described that include secondary microcephaly as a feature continues to grow, for example, the newly defined and linked cerebellar atrophy with progressive microcephaly (CLAM) form of pontocerebellar hypoplasia (Rajab *et al.,* 2003). Children with secondary microcephaly has a normal head size at birth, with a later decrease in the rate of growth, which results in a small head size in later childhood. It is probably caused by decreased dendritic connection/ activity of a (near) normal number of neutrons. Secondary cases were generally characterized by convulsions, spasticity, and other congenital anomalies. Rett syndrome is one of the most common and best known of the secondary microcephalies. Rett syndrome is a disorder of brain development that occurs almost exclusively in girls. Brain size and neurological function are apparently normal until the onset of the disease at 6-18 months (Shahbazian *et al.,* 2002). The

developmental regression occurs coincident with a reduction in brain growth, which results in severe mental retardation and frequent seizures. The condition occurs almost exclusively in females and is due to mutations in an apparently ubiquitously expressed X-linked gene, methyl-CpG-binding protein2 (*MECP2;*MIM 300005), a transcriptional repressor methyl CpG binding protein involved in gene silencing (Shahbazian *et al.,* 2002).

Clinical Features of Autosomal Recessive Primary Microcephaly

Brains of the individuals with Autosomal Recessive Primary Microcephaly (MCPH) are characterized by a substantial reduction in size of the cerebral cortex and a generalized reduction in size of the remainder of the nervous system, but with normal architecture (Mochida and Walsh, 2001). The child affected by MCPH is microcephalic at birth but during early stages of development in the first year of life are often normal. After the first year of life, development is only mildly delayed but progress in speech is usually delayed. Head circumference (HC) is used as a surrogate measurement of brain size; however, it is only imperfectly correlated with brain volume. Other methods have been used (e.g., volumetric nuclear magnetic resonance [NMR] scanning), but HC remains the common, simple method for evaluating gross brain size (Aicardi, 1998). An HC of three standard deviations below the mean (−3 SD) is usually the cut-off for defining microcephaly (Ross and Frias, 1977; Baraitser, 1990).

Microcephaly is strongly correlated with mental retardation (Dolk, 1991). All individuals with MCPH have mild to moderate mental retardation. Motor and social milestones are mildly delayed but speech development is consistently delayed. There is no evidence of progressive cognitive decline or any motor deficit with age (Roberts *et al.*, 2002). Some individuals, which may have reduction in height, but the head circumference will always be significantly more reduced than height (Neitzel *et al.*, 2002; Trimborn *et al.*, 2004). There are no major dysmorphic features except facial characteristics of a hypoplastic skull vault and sloping forehead, which is not always present. In rare cases patients may present with seizures (Shen *et al.,* 2005). Craniosynostosis (premature fusion of skull sutures) is not a feature of microcephaly.

Causes of Microcephaly

There are many nongenetic and genetic causes of "microcephaly with mental retardation". The non-genetic reasons are; maternal alcohol consumption during pregnancy, maternal syphilis infection, inadequate gestational weight gain or poor prenatal care, non-accidental head injury, lack of proper vitamins and nutrients in the diet, maternal diabetes, exposure to radiations i-e maternal x-ray analysis during pregnancy, intrauterine exposure to teratogenic agents. There are environmental causes and some genetic aetiologies due to mechanisms, including cytogenetic abnormalities, single gene disorders, etc.

Incidence of MCPH

Autosomal recessive microcephaly was reported to have an incidence of 1/30,000 in Japan, 1/250,000 in Holland, and 1/2,000,000 in Scotland (Tolmie *et al.*, 1987). More-recent studies have not been performed; however, MCPH seems rarer in whites than in Asian and Arab populations (one in 10,000 in Northern Pakistanis) where consanguineous marriage is practiced (Woods *et al.*, 2005). An increased incidence of autosomal recessive diseases in consanguineous populations is expected on theoretical grounds and has been observed (Alam, 1993; Tuncbilek, 2001). Given the number of MCPH genes and mutations found in the Pakistani population, the high incidence of MCPH probably reflects the effects of consanguinity and not a founder effect.

Molecular Genetics of Primary Microcephaly (MCPH)

Pattern of Inheritance

The pattern of inheritance in families with primary microcephaly is predominantly autosomal recessive. The expected recurrence risk for autosomal recessive traits is one in four, the empiric recurrence risk for a nonconsanguineous couple who have had one child with a diagnosis of MCPH has been calculated as one in five (Tolmie *et al.*, 1987). Autosomal dominant and X-linked inheritance for primary microcephaly is also reported; however, no loci for these have yet been reported.

Genetic Heterogeneity

MCPH appears to be a single definable clinical entity; however, genetic heterogeneity has been shown. To date, eight different loci (MCPH1–MCPH8) for primary microcephaly have been mapped (Jackson *et al.,* 1998; Roberts *et al.,* 1999; Jamieson *et al.,* 1999; Moynihan *et al.,* 2000; Pattison *et al.,* 2000; Leal *et al.,* 2003). Four of the six loci (MCPH1– MCPH3 and MCPH5) were originally discovered in families of northern Pakistani origin (Jackson *et al.,* 1998; Moynihan *et al.,* 2000; Jamieson *et al.,* 2000), while MCPH4 and MCPH6 were discovered in the Moroccan and Brazilian families, respectively (Jamieson *et al.,* 1999; Leal *et al.,* 2003). Two other loci MCPH7 and MCPH8 have been discovered by Woods group at Cambridge University, UK but the results have not been published yet (Personal communication).

MCPH heterogeneity studies have been performed and showed that MCPH5 is the most common locus so far, accounting for linkage of nearly half of the amassed families of Pakistani origin (Roberts *et al.,* 2002, Gul *et al.,* 2006).

Genetic Loci/Genes

MCPH1 Locus

First locus for primary microcephaly, MCPH1, was mapped, to chromosome 8p23 by homozygosity mapping in two consanguineous families originating from the Mirpur region of northern Pakistan (Jackson *et al.,* 1998). To identify the causative gene in a form of primary microcephaly linked to chromosome 8p23, Jackson *et al.* (2002) sequenced *Microcephalin* gene, which was previously uncharacterized, and showed a nonsense mutation in two families sharing the ancestral 8p23 haplotype.

Microcephalin

Microcephalin (MIM 607117) has been identified to be responsible for Primary microcephaly at MCPH1 locus. Mutations have been identified in *Microcephalin* gene to cause MCPH. It has 14 exons, spanning a length of 241 kb in the human genome. Microcephalin consists of 835 amino acids and is predicted to contain three BRCA1 C-terminal (BRCT) domains. One BRCT domain is present at the N-terminus and two at the C-terminus of Microcephalin. These domains interact to form homo/hetero BRCT

multimers (Huyton *et al.*, 2000). It shares only 57% identity with its mouse ortholog, with the most conserved regions being the BRCT domains, where there is 80% identity. The closest homologues of MCPH1/microcephalin are BRCA1 and topoisomerase II binding protein, owing to their shared BRCT domains. These BRCT domains are known to be present in several key proteins controlling the cell cycle. Therefore, mutation in microcephalin may cause primary microcephaly by perturbing normal cell-cycle regulation in neural progenitors (Huyton *et al.*, 2000).

To date, four mutations have been reported in Microcephalin gene causing MCPH and an allelic form, Premature chromosome condensation syndrome (PCC; MIM 606858), characterized by microcephaly, short stature, and misregulated chromosome condensation. Jackson *et al.* (2002) reported the first mutation, a nonsense mutation (c.74G>C; Ser25X), in exon 2 of *Microcephalin* gene in two Pakistani families with an identical haplotype. Trimborn *et al.* (2004) studied a Lebanese family, and found a homozygous 1bp insertion mutation (c.427_428insA), leads to a frameshift resulting in a premature stop codon in exon 6 of *MCPH1* gene. Trimborn *et al.* (2005) reported a homozygous substitution of a highly conserved threonine residue by an arginine (c.80C>G, Thr27Arg) in the N-terminal *BRCT* domain of *MCPH1*.

Using RT-PCR of fetal tissues, Jackson *et al.* (2002) confirmed that *microcephalin* is expressed in fetal brain. The expression pattern of Microcephalin in the brain is consistent with a role in neurogenesis and in regulation of the size of the cerebral cortex. Microcephalin functions as a proximal factor in the DNA damage checkpoints that control multiple damage sensors and early mediators and also implicated in cell cycle checkpoints, controlling and regulating other important molecules and thus affecting the timing of mitosis; its depletion abolishes the DNA damage response and results in centrosomal abnormalities and chromosomal aberrations (Lin *et al.*, 2005; Alderton *et al.*, 2006; Chaplet *et al.*, 2006).

MCPH2 Locus

Roberts *et al.* (1999) studied two consanguineous families, and described the identification of a second novel locus for autosomal recessive primary microcephaly, MCPH2, located at chromosome 19q13.1–13.2, confirming genetic heterogeneity for this

condition. The minimum critical region containing the MCPH2 locus was defined by the polymorphic markers D19S416 and D19S420, spanning a region of approximately 7.6 cM. The causative gene for MCPH2 has yet not been identified.

MCPH3 Locus

Third locus for MCPH (MCPH3) was identified by homozygosity mapping of a consanguineous Pakistani family. The region of homozygosity identified in all microcephalic individuals was on chromosome 9q34 (Moynihan *et al.,* 2000). Mutations have been identified in *CDK5RAP2* gene in families with primary microcephaly.

CDK5RAP2

Mutations in Cyclin-dependent protein kinase 5, regulatory subunit associated protein 2, (*CDK5RAP2;* MIM 608201) gene at MCPH3 locus are least involved in causing MCPH phenotype. To date only three families showed linkage to MCPH3 locus at chromosome 9q34. Bond *et al.* (2005) have reported two homozygous mutations (243T>A and IVS26-15A>G) in *CDK5RAP2* gene in two families from Pakistan linked to MCPH3 locus. A homozygous mutation in the *CDK5RAP2* gene was identified in affected members of each of the 2 families. Recently, Hassan *et al.* (2007) reported the identification of a previously described nonsense mutation (243 T>A S81X) in exon 4 of *CDK5RAP2* gene in a Pakistani family of Kashmiri origin.

The gene *CDK5RAP2* has a genomic size of 191290 bps and contains 34 exons, with a deduced open reading frame of 6230 bps and 1893 translated residues (Bond *et al.,* 2005; Evans *et al.,* 2006). The *CDK5RAP2* gene has predicted to contain one N-terminal spindle associated domain and two potential chromosome segregation ATPase (SMC, structural maintenance of chromosomes) domains, which are known to play a role in the cohesion and condensation of chromosomes during mitosis (Cox *et al.,* 2006). RT-PCR ELISA detected moderate to high expression of *CDK5RAP2* in all tissues and specific brain regions examined. Highest levels were detected in skeletal muscle, fetal liver, brain, kidney, and ovary. Within specific brain regions, highest expression was detected in thalamus, corpus callosum, substantia nigra, hippocampus, and caudate nucleus.

CDK5RAP2 was initially identified in a rat brain yeast-2-hybrid search for rat cerebral cortex proteins interacting with cyclin-dependent kinase 5 regulatory protein 1 (CDK5R1) (Ching *et al.*, 2000; 2002). CDK5R1 activates cyclin dependent kinase 5 (CDK5). CDK5 has been shown to be structurally and functionally related to the cyclin-dependant kinase family, but is not involved in control of the cell cycle. CDK5 is a promiscuous protein kinase only functioning in the brain and with numerous neuronspecific roles in processes including neurogenesis, neural migration and neurodegeneration (Kesavapany *et al.*, 2004). *CDK5RAP2* has a potential role in the inhibition of centrosomal CDK5 during neurogenesis. Its localization to the spindle poles of mitotic cells suggests involvement of a centrosomal mechanism during mammalian brain development (Bond *et al.*, 2005).

However, *CDK5RAP2* function in mammals has not been elucidated. Bioinformatics gives little assistance in predicting functional protein domains but does reveal a potential orthologue in Drosophila, Centrosomin (Bond *et al.*, 2005; Woods *et al.*, 2005), and a homologue in mammals, Myomegalin. Immunohistochemistry and confocal microscopy of N-terminal antibodies in HeLa cells showed presence of CDK5RAP2 at centrosome throughout mitosis and it has been hypothesized that an unidentified centrosomal mechanism controls the number of neurons generated by neural precursor cells (Bond *et al.*, 2005). Therefore, *CDK5RAP2* is hypothesized to affect neurogenic mitosis by reducing the availability of the microtubules that are needed to build the mitotic spindle and astral microtubule network and that might regulate neural progenitor cell division and cell number (Cox *et al.*, 2006; Tang, 2006).

MCPH4 Locus

Jamieson *et al.* (1999) reported the mapping of a fourth locus for primary microcephaly, MCPH4, at chromosome 15q15-q21 in a consanguineous Moroccan family. Haplotype analysis of the MCPH4 provided a maximum multipoint LOD score of 3.29. The causative gene for MCPH4 has yet not been identified.

MCPH5 Locus

The fifth novel locus for autosomal recessive primary microcephaly, MCPH5, was mapped to chromosome 1q31 by two separate research groups. In a family of Turkish

origin, Jamieson *et al.* (2000) mapped the MCPH5 locus to a 11.4 cM region at chromosome 1q25-q32. Simultaneously and independently, Pattison *et al.* (2000) studied a large consanguineous Pakistani family, and determined by linkage mapping that an MCPH5 locus is located on chromosome 1q31. Bond *et al.* (2002) adopted a positional cloning strategy to identify the gene mutant in at MCPH5 locus. They identified the abnormal spindle-like microcephaly-associated (*ASPM*) gene within a 600-kb region defined by common haplotypes in 4 consanguineous northern Pakistani families with primary microcephaly. Mutations in the *ASPM* gene at the MCPH5 locus appear to be the most common cause of autosomal recessive primary microcephaly.

ASPM

The abnormal, spindle-like, microcephaly-associated (*ASPM;* MIM 650481) gene is the human ortholog of the Drosophila melanogaster 'abnormal spindle' gene (*asp*), which is essential for normal mitotic spindle function in embryonic neuroblasts (Bond *et al.*, 2002). Bond *et al.* (2002) reported the first mutation, a homozygous mutation, in *ASPM* gene at MCPH5 locus in four consanguineous northern Pakistani families with primary microcephaly, leading to premature stop codon into the predicted *ASPM* open reading frame. *ASPM* gene is composed of 28 exons and spans 62 kb on the genomic sequence with a 10,434-bp ORF and encodes 3,477 amino acids.

ASPM comprises an amino terminal microtubule binding domain (Saunders *et al.*, 1997), a calponin homology domain, 74 isoleucine-glutamine (IQ) domains (which potentially bind calmodulin) (Craig and Norbury, 1998; Bond *et al.*, 2002), and a carboxy-terminal region with no identified domains. It has been shown that most IQ motifs are organized into a higher order trimer repeat (HOR) containing two 23-amino acid residue units and one 27-amino acid residue unit (Kouprina, 2005). The predicted ASPM protein is conserved between human, mouse, Drosophila, and worm, with a consistent correlation of nervous-system complexity and protein length, principally involving an increase in the number of encoded IQ domains (Bond *et al.*, 2002).

The function of human *ASPM* has been proposed on the basis of the analysis of Drosophila mutants with a deficiency in the asp gene (Avides and Glover, 1999; Avides *et al.*, 2001; Bond *et al.*, 2002). The Drosophila asp gene encodes a 220 kDa microtubule

associated protein found at the spindle poles and centrosomes from prophase through early telophase. Asp is co-purified with g-tubulin from centrosomes and both are required for the organization of microtubules into asters (Avides and Glover, 1999). Together, these observations suggest that mutations in human *ASPM* may cause microcephaly due to the disregulation of mitotic spindle activity in neuronal progenitor cells.

Horvath *et al.* (2006) identified *ASPM* as a highly connected 'hub' gene within a module of mitosis/cell cycle genes that are coexpressed in glioblastoma and breast cancer. They demonstrated *ASPM* overexpression in glioblastoma compared to normal tissues. *Aspm* expression was also high in fetal murine neural stem/progenitor cells, and its expression decreased during differentiation. Knockdown of *ASPM* by small interfering RNA inhibited proliferation in both a human glioblastoma cell line and murine neural stem/progenitor cells.

ASPM was found to be concentrated at mitotic spindle poles in mouse neuroepithelial cells, the primary stem and progenitor cells of the mammalian brain (Fish *et al.,* 2006). Upon RNA interference in telencephalic neuroepithelial cells, Aspm mRNA was reduced, mitotic spindle poles lacked Aspm protein, and the cleavage plane was less frequently oriented perpendicular to the ventricular surface of the neuroepithelium. The alteration in the cleavage plane orientation increased the probability that the cells underwent asymmetric division, i.e., the apical plasma membrane was inherited by only 1 of the daughter cells. Fish *et al.* (2006) concluded that ASPM protein is crucial for maintaining a cleavage plane orientation that allows symmetric, proliferative division of neuroepithelial cells during brain development and in turn brain size.

Several mutations have been reported in the *ASPM* gene so far, which are the most common cause of MCPH in Pakistani and other world populations, including those of Turkey, Yemen, Saudi Arabia, Jordan, the Netherlands, and India (Bond *et al.,* 2002; 2003; Kumar *et al.,* 2004; Shen *et al.,* 2005; Gul *et al.,* 2006; 2007).

MCPH6 Locus

Leal *et al.* (2003) mapped the sixth locus for autosomal recessive primary microcephaly, MCPH6, to chromosome 13q12.2 in a Brazilian family. Bond *et al.* (2005) used a positional cloning strategy to identify candidate genes in the region. Bioinformatic

analysis of the region identified a gene, centromeric protein J (*CENPJ*). Mutations in the *CENPJ* gene underlie the cause of primary microcephaly at MCPH6 locus.

CENPJ

The centromeric protein J (*CENPJ;* MIM 609279), also known as centrosomal protein 4.1-associated protein (CPAP), is one of the more recently identified MCPH genes. To date, only three mutations including two deletion mutations and a missense mutation have been identified in the *CENPJ* gene. In affected members of 3 families with MCPH6, of which 1 was the Brazilian family previously described by Leal *et al.* (2003) and 2 were Pakistani, Bond *et al.* (2005) identified a homozygous single base deletion mutation 17delC resulting in a premature stop codon (T6fsX3) and a missense mutation (E1235V) in the *CENPJ* gene. Recently, Gul *et al.* (2006) identified a 4-bp deletion, c.3,243–3,246delTCAG, in the *CENPJ* gene in a Pakistani family with autosomal recessive primary microcephaly.

This gene contains 17 exons and spans 40 kb on human chromosome 13q. Analysis of cDNA of *CENPJ* revealed a nucleotide sequence of 4,370 bases that contains a single open reading frame (ORF) of 1,338 amino acids (Hung *et al.,* 2000). This ORF starts at position 211 with an in-frame ATG and ends with a translation stop codon, TGA, located at nucleotide position 4225. The *CENPJ* shows high level of expression in brain and spinal cord with primary expression localize to neuroepithelium (Bond *et al.,* 2005).

The *CENPJ* protein is a centrosomal protein localized to centrosomes in interphase and to the spindle poles during mitosis (Hung *et al.,* 2000). The CENPJ protein consists of multiple hydrophobic regions and a C-terminal domain (residues 978–1,338) that shares limited homology with human Tcp-10, which is a t-complex responder gene that plays a role in the sex transmission ratio distortion. The hydrophobic regions in *CENPJ* form a stripe that winds around alpha-helix, which is capable of interacting with the hydrophobic residues of a second molecule to form a coiled-coil structure (Cohen and Parry, 1986; Hung *et al.,* 2000). Several recent reports have shown that *CENPJ* contributes in the RelA, STAT5 and NF-kB mediated transcription, but these seem less likely to influence neurogenesis (Peng *et al.,* 2002; Koyanagi *et al.,* 2005; Bond and Woods, 2006).

Recently, Cho *et al.* (2006) have observed that depletion of CPAP disrupts centrosome integrity, and cells lacking CPAP arrest in mitosis with multipolar spindles.

Hung *et al.* (2000) concluded that CPAP is a centrosomal protein that may have a role in microtubule nucleation. The 4.1R protein non-erythrocyte 135 splice variant (4.1R-135) serves as an adaptor that anchors the *CENPJ*/g-tubulin complex to the centrosome. The N-terminus of 4.1R-135 interacts with the C-terminal Tcp10 domain of *CENPJ*, and *CENPJ* is associated with the g-tubulin ring complex (Hung *et al.*, 2004). In vitro evidence shows that *CENPJ* can inhibit microtubule nucleation from the g-tubulin ring complex and is also able to depolymerise Taxol-stabilised microtubules (Hung *et al.*, 2004). While a single *CENPJ* gene exists in other species, including Drosophila, to date the mutant phenotype has only been described in man. RNAi knockdown of *CENPJ* arrests all cells during mitosis and many of them have multi-polar spindles (Cho *et al.*, 2006). However, it is surprising that MCPH individuals with MCPH6/*CENPJ* truncating mutations do not have a more general growth-deficiency phenotype. The RNAi-*CENPJ* spindle poles contained the normal centrosomal compo-nents NUMA, g -tubulin and Aurora-A.

Other functions of *CENPJ* are as a coactivator of NF-kB-mediated transcription and to augment Stat5-mediated transcription, but these seem less likely to influence neurogenesis (Peng *et al.*, 2002; Koyanagi *et al.*, 2005). This indicates *CENPJ* protein might have an important role in centrosome duplication at the beginning of mitosis that might regulate neural progenitor cell division and cell number (Leidel and Gonczy, 2005; Tang, 2006).

MCPH7 and MCPH8 Loci

These two loci have been discovered by Woods group at Cambridge University, UK but the results have not been published yet. A gene, Inositol polyphosphate-5-phosphatase E (*INPP5E*) has been identified at MCPH7 locus on human chromosome 9q34.3 (Personal communication).

INPP5E

Inositol polyphosphate-5-phosphatase E (INPP5E) gene contains 10 exons and spans 11 kb on human chromosome 9q34.3. The protein encoded by this gene is an inositol 1, 4, 5-trisphosphate (InsP3) 5-phosphatase. InsP3 5-phosphatases hydrolyze Ins (1, 4, 5) P3, which mobilizes intracellular calcium and acts as a second messenger mediating cell responses to various stimulation. Studies of the mouse counterpart suggest that this protein may hydrolyze phosphatidylinositol 3, 4, 5-trisphosphate and phosphatidylinositol 3, 5-bisphosphate on the cytoplasm Golgi membrane and thereby regulate Golgi-vesicular trafficking.

In the present study genotyping using microsatellite markers was performed in four consanguineous Pakistani families with MCPH collected from different regions of Pakistan. Three of the four families (A, B and C) showed linkage to MCPH5 locus while family D showed linkage to MCPH7 and were further subjected to sequencing analysis to delineate pathogenic mutations in the *ASPM* and *INPP5E* genes.

MATERIALS AND METHODS

MATERIALS AND METHODS

Families Studied

For the study, presented here, four families (A, B, C, D) with autosomal recessive primary microcephaly (MCPH) were ascertained from different regions of Pakistan. The families were visited at their places of residence to generate pedigrees and collect other relevant information. Informed consent was obtained from parents, of the affected children, and all other family members who participated in the study. Written consent was also taken from the parents/guardians of the affected children to publish their photographs. Information regarding medical and family history of each family was collected. Head circumference of each affected and normal members was measured. Presence or otherwise of any dysmorphic features in the affected members were noted and their mental status was evaluated. Photographs of each individual assessed to be affected were taken. Blood samples from affected and normal individuals of each family were collected for DNA extraction.

Pedigree Analysis

For genetic implication an extensive pedigree was constructed for each family by the standard methods described by Bennett *et al.* (1995). The pattern of inheritance of the disease was deduced by observing the mode of segregation or transmission within family. The exact genealogical relationships of all the affected individuals were obtained through extensive personal interviews of elders of the families. Males were symbolized by squares and females by circles. The normal individuals were designated with unfilled symbols while the affected individuals by filled symbols. Each generation was indicated by Roman numeral. The individuals within a generation were designated by Arabic numerals. A number enclosed within a symbol indicates the number of sibs (males or females), as the case may be.

Blood Sampling

Blood samples from both affected and normal members of the families were collected using 10 ml syringes (0.7 X 40 mm, 22 G X 1 1/2) and vacutainer tubes containing potassium EDTA. The blood samples collected were stored at 4°C.

Extraction and Purification of Genomic DNA

Genomic DNA was prepared by standard phenol/chloroform method. Approximately 0.75 ml of blood was taken in a micro-centrifuge tube along with 0.75 ml solution A and was kept at room temperature for 5-10 minutes after mixing the contents. The tube was then centrifuged for 1 minute at 13,000 rpm and after discarding the supernatant the pellet was resuspended in 400 µl of solution A. Centrifugation was repeated and after discarding the supernatant the nuclear pellet was resuspended in 400 µl of solution B, 12 µl of SDS and 25 µl of proteinase K and incubated at 37°C over night. On the following day 0.5 ml of a fresh mixture of equal volume of solution C and D was added in sample, mixed and centrifuged for 10 minutes at 13,000 rpm. The aqueous phase (upper layer) was collected in a new tube and equal quantity of solution D was added. Centrifugation was then carried out again at 13,000 rpm for 10 minutes. The aqueous phase was placed in a new tube and after adding 55 µl of 3 M sodium acetate (pH 6) and equal volume of isopropanol. Tubes were then inverted several times to precipitate DNA. The DNA pellet was washed with chilled 70% ethanol and dried in the incubator at 37°C. After evaporation of residual ethanol, DNA was dissolved in appropriate amount of DNA dissolving buffer.

Composition of Solutions

Solution A

0.32 M Sucrose

10 mM Tris (pH 7.5)

5 mM $MgCl_2$

1 % (v/v) Triton X-100

Solution B

10 mM Tris (pH 7.5)

400 mM NaCl

2 mM EDTA (pH 8.0)

Solution C

400 µl Phenol

10 mM Tris

Solution D

Chloroform 24 volumes

Isoamyl alcohol 1 volume

DNA Dissolving Buffer

10 mM Tris (pH 8.0)

1 mM EDTA

Genomic DNA Preparation by Commercially Available Kit

DNA extraction was also carried out using Genomics isolation Kit (Sigma Chemical Co. USA). One hundred and fifty microlitre of blood was taken in a 1.5 ml microcentrifuge tube along with 250 µl of lysis solution A; mixed by inversion, incubated at 65°C for 6 minutes. Clear aqueous phase was transferred to a new 1.5 ml microcentrifuge tube after adding 100 µl of precipitation solution B and centrifugation at 14,000 rpm for 5-10 minutes. DNA was then precipitated by adding 500 µl of 100% ethanol. Ethanol was removed after centrifugation at maximum speed for 2 minutes, and then washed with chilled 70% ethanol. After evaporation of residual ethanol DNA was dissolved in appropriate amount of Tris-EDTA (TE) buffer by incubation at 65°C for 5 minutes.

DNA Dilution and Micropipetting

Genomic DNA was quantified by taking optical density (OD) at 260 nm wavelength by using GeneRay UV-Photometer (Biometra®, Germany). and subsequently diluted to 40-50 ng/µl for PCR amplification. Micropipetting was carried out by using adjustable micropipettes with autoclaved disposable tips, ranging from 10-1000 µl of upper volume limit.

Genotyping

The analysis of microsatellite markers was performed by PCR; the amplified products were resolved on 8% standard non-denaturing polyacrylamide gel as described above. Microsatellite markers were visualized by placing the ethidium bromide stained gel on UV transilluminator and genotypes were assigned by visual inspection of the gels. Microsatellite markers mapped by Cooperative Human Linkage Centre (CHLC), were

obtained from Research Genetics, Inc. (USA). The cytogenetic locations of these markers, their hetrozygosity as well as the length of the amplified products were obtained from genome database homepage (www.gdb.org) and Marshfield Medical Center (www.marshmed.org/gentics/).

Linkage to Known MCPH Loci

To elucidate the gene defect in the families, presented here, an initial search for linkage was carried out by using polymorphic markers mapped within all seven known autosomal recessive primary microcephaly loci. Average heterozygosity of each marker was above 70%, implying that these markers are highly informative for allelotyping pedigree members.

Table 2.1 summarizes microsatellite markers located in the region of known MCPH loci, which were used as first pass analysis for the genetic linkage in the families with autosomal recessive primary microcephaly. Genotyping of these markers was performed as described above.

Polymerase Chain Reaction (PCR)

PCR amplification of the microsatellite markers was performed according to standard procedures in a total volume of 25 ul, containing 40 ng genomic DNA, 20 pmol of each primer, 200 uM of each deoxyribonucleotide triphosphate, 1 U of Taq DNA polymerase (MBI Fermentas, Sunderland, UK), and 1× PCR buffer (MBI Fermentas, UK). PCR was carried out for 35 cycles, with the following thermal cycling conditions: 95°C for 1 min, 57°C for 1 min, and 72°C for 1 min, followed by a final extension at 72°C for 7 min in a thermal cycler 9600 (Perkin Elmer, Wellesley, MA, USA).

Agarose Gel Electrophoresis

Amplified PCR products were analyzed on 1-2% agarose gel, which was prepared by melting 1-2 grams of agarose in 100 ml 1X TBE buffer (0.89 M Tris, 0.025 M Borate, 0.032 M EDTA pH 8.3), in a microwave oven for few minutes. Ethidium bromide (final concentration 0.5 μg/ml) was added to the gel to facilitate visualization of DNA after electrophoresis. PCR reaction products were mixed with Bromophenol Blue dye (0.25% Bromophenol Blue in 40% sucrose solution) and loaded into the wells. Electrophoresis was performed at 100 volts for half an hour in 1X TBE buffer.

Amplified products were detected by placing the gel on UV Transilluminator (Biometra, Germany).

Polyacrylamide Gel Electrophoresis

The amplified PCR products were resolved on 8% non-denaturing polyacrylamide gel. Reagents were mixed in a flask and polyacrylamide gel solution was poured between two glass plates held apart by spacers of 1.5 mm thickness. After inserting the comb, gel was allowed to polymerize for 20-30 minutes at room temperature. Amplified products were mixed with loading dye containing 0.25% bromophenol blue prepared in 40% sucrose solution and loaded into the wells. Electrophoresis was carried out at 100 volts for 90 minutes and the gel was stained with ethidium bromide (10 mg/ml) solution for visualization on UV Transilluminator. Gel was photographed by using Digital camera DC 120 (Kodak, USA).

Composition of 8% Polyacrylamide Gel

13.5 ml 30% Acrylamide solution (29 g acrylamide, 1g N, N Methylene-bis-acrylamide). 5 ml 10X TBE; 0.35 ml 10% Ammonium persulphate; 17.5 µl TEMED; 31.13 ml distilled water.

Mutation Screening in *ASPM* gene

For screening *ASPM* gene, all 28 exons spanning 62 kb on the gene map, including their intron-exon boundaries were amplified by PCR from genomic DNA of affected individuals of families A, B and C, which were linked to MCPH5. The amplified products were directly sequenced in automated DNA sequencer ABI 310. The primer sets used for amplification of *ASPM* exons are given in Table 2.2.

Mutation Screening in *INPP5E* gene

For screening *INPP5E* gene, all 10 exons spanning 11 kb on the gene map, including their intron-exon boundaries were amplified by PCR from genomic DNA of affected individuals of family D, which were linked to MCPH7. The primer sets used for amplification of *INPP5E* exons are given in Table 2.3.

DNA Sequencing

To delineate any pathogenic mutations in the *ASPM* and *INPP5E* genes, DNA sequencing of affected individuals was carried out according to DNA sequencing

protocol. Thermo-cycling conditions were same as described above. The concentration of genomic DNA was 100 ng and the concentration of primers used was 2.5 µl (20 ng/µl) in 25 µl of reaction mixture. PCR products were analyzed on 2% agarose gel along with 100 bp DNA Ladder (O Range Ruler™, MBI Fermentas, UK). The amplified products were purified using Rapid PCR purification Kit (Marligen, USA). Three hundred micro liters of binding solution (H1) (concentrated Guanidine HCl, EDTA, Tris-HCl, and Isopropanol) was added to the amplification reaction and mixture was applied to a spin cartridge containing silica-based membranes where the double stranded DNA was selectively adsorbed. Adsorption to the membrane is influenced by buffer composition and temperature. DNA polymerase, buffer, unreacted primers and dNTPs were removed with 500 µl of alcohol-containing wash buffer (H2) (NaCl, EDTA, Tris-HCl). DNA was eluted in Tris-EDTA buffer (10 mM Tris-HCl (pH 8.0), 0.1 mM EDTA) at 70°C. Purified products were subjected to cycle sequencing using Big Dye terminator V 3.1 ready reaction mixed and sequencing buffer (PE Applied Biosystems, Foster city, CA, USA). The reaction mixture was taken through thermocycling conditions consisting: 5 minutes of 95°C for template DNA denaturation followed by 30 cycles of amplification each consisting of 3 steps: 30 seconds at 95°C for DNA denaturation into single strands; 30 seconds at annealing temperature (same as in amplification PCR) for primers to hybridize or "anneal" to their complementary sequences; 4 minutes at 72°C for extension of complementary DNA strands from primers; 10 minutes at 72°C for Taq DNA polymerase to synthesize any unextended stands left (single cycle).

The sequencing products were purified by ethanol precipitation protocol (POP6 Protocol). Sequencing products were transferred to 1.5 ml microcentrifuge tube, containing 16 µl of distilled water and 64 µl 100% ethanol. Tubes were kept at room temperature for 15 minutes, and centrifuge at 14,000 rpm for 20 minutes. Supernatant was removed and 250 µl of 70% ethanol was added into the tubes. Tubes were centrifuged at 14,000 rpm for 10 minutes after thorough mixing. Supernatant was discarded and 20 µl of T.S.R. (Template Suppression Reagent) was added into the tube. Mixture thus obtained was placed in 0.5 ml septa tube.

After applying denaturation temperature of 95°C for 2 minutes, the samples were sequenced through Automated Genetic Analyzer, ABI Prism 310® (Applied Biosystem, USA). The chromatograms of the affected individuals were compared

with the corresponding control gene sequences from Ensemble Genome Browser database to identify the any nucleotide base pair change (http://www.ensembl.org/index.html).

Table 2.1: List of microsatellite markers used for linkage to known MCPH loci

Locus	Cytogenetics location	Marker	Distance (cM) Rutgers Map Build 36	Amplified Length (bp)	Polymorphism
MCPH1	8p22_ pter	D8S518	9.88	245	DNR
		D8S1798	11.96	165	DNR
		D8S1099	12.46	253	TriNR
		D8S1742	13.72	242	TNR
		D8S277	14.92	180	DNR
		D8S561	15.04	172-182	DNR
MCPH2	19q13-13.2	D19S719	55.67	249	TetNR
		D19S416	56.28	173	DNR
		D19S220	62.62	265-283	DNR
		D19S223	66.09	228	DNR
		D19S197	67.72	153	DNR
		D19S537	69.1	164	DNR
MCPH3	9q34	D9S1776	123.79	131	DNR
		D9S1872	128.65	135	DNR
		D9S1850	131.56	230	DNT
		D9S1881	135.52	220	DNR
		D9S290	139.74	156	DNR
		D9S1831	142.79	239	DNR
MCPH4	15q15-21	D15S118	32.39	230	DNR
		D15S641	41.37	105	TriNR
		D15S126	47.92	218	DNR
		D15S962	51.59	282	DNR
		D15S117	55.04	150	DNR
		D15S527	58.51	400	TNR
MCPH5	1q25-32	D1S3468	205.4	302	TNR
		D1S518	205.55	197	TNR
		D1S2823	207.86	131	DNR
		D1S2625	208.26	185	DNR
		D1S408	210.78	182	TNR
		GATA135FO2	211.73	164	MSR

		D1S1183	211.89	182	DNR
		D1S2816	211.89	250	DNR
		D1S1660	213,11	239	TNR
		D1S1726	213.8	275	DNR
		D1S2716	215.44	196	DNR
MCPH6	13q12.2	D13S1275	6.97	198	DNR
		D13S787	8.75	251	TNR
		D13S742	11.71	364	TNR
		D13S1294	13.94	247	DNR
		D13S1304	16.05	149	DNR
		D13S1242	21.27	248	DNR
MCPH7	9q34.3	D9S1818	152.82	151	DNR
		D9S1826	160.5	133	DNR
		D9S158	163.08	213	DNR
		D9S905	165.2	294	TetNR
		D9S2168	167.16	122	unknown

cM: centiMorgan; bp: base pair

Table 2.2: List of primers used in screening *ASPM* gene

Exon No.	PRIMER (5′→3′)		Product Size *(bp)	Annealing Temp (°C)
	Forward	Reverse		
1	TTCACTCCCACGACCTCTAC	TCTCCAATCGTCAACCTTCC	472	58
2	GAGACTATCTGTTCTATTGC	TAATGGTATCCCAAAGACTC	570	52
3-1	ACTAGGAAATGCAGAAGAGC	AAGGAAGTTTCAGTTACAGC	560	51
3-2	AATGAATGCCATGGTGCAAC	GCTTTGGGAGATTTTGAACC	672	51
3-3	AGATAATTCACAGCCTGTGC	TTTTCATGTTCACCCACTGC	575	52
3-4	CGTCCAATACTTTCTGCCAC	GCTAAGGAAATGTACCCAGC	582	55
4	GGTTTATGGTCTGTGACTTC	AGTTGACACAATATCCTGTC	458	52
5	AAATGCTTTCAGCTCTTTCC	AATGAACAGGGAATTATGCC	380	58
6	AGATTGGCCTAAGGAGTAAG	ATATGCCAGTTTTACCTGTC	458	58
7	TTCCCACTGATATACTCTCC	TTGTCATTACGTGCAACACC	478	53
8	TCCTTAGGTTATGGTCTGCC	GAAGGGAGAGTACTAGAAGC	330	58
9	TTTATTTGTGCTTGCTACCC	GCATTCCTATTTTACTCCTC	352	58
10	GAGCAACTTTTAGAAAGATC	ATTGTACTACTTGAAAGAGC	422	58
11	TAAGAACTCTACTTGCCGAC	TTTTCTCTGTGCCTATCCAC	450	53
12	GAATTAAGTGATGAGCATGG	TTACTGGGGCAAAATAAACC	282	58
13	TCAGTGTAGATGGTGTTTGC	GAGGGAAAGTTTGCTTACAC	540	58
14	CCTTGTAGATTTGTCACTCC	AAGGAGAAATTAGCCGTAGC	394	53
15	CAGTTCTCTGGATATGTCTC	GTTGTTTGTATGAGTCGAGC	468	53
16	CAGAAGATGATAGTAAGTAC	CTTAATAATGCCATACATCC	306	49
17	TGTAGGGGTGTTTTATTTCC	CTTCATCACATTTTGCCTTC	395	51
18-1	GAATTGGCTACAGGTATATC	GGTTAGTATGGACACTTTTC	422	50
18-2	AAGAGCTTTTAGAGAATGGC	TCATCTTAACAGTTGACTGC	725	50
18-3	GCATATAGAGGGATGCAAGC	TGGCCATTCTAAAAGCAGAC	812	55
18-4	ATTCAGAGATGGTACAGGGC	TCAGGTACTTTTCACGCTGC	924	55
18-5	ATTCAACACATGCACAGGGC	GTCTGAGATAATGCTGCCTC	814	55
18-6	AAAGGATGCGAGAGATGCAC	TAATAATGGCAGCCTGGTGC	906	55
18-7	ATCAGACAATGGCATTCTGC	ATACTCTGCTTCCTGTGAAC	852	53
18-8	GTACGAACTATTCAGGCTGC	TTACTAGTGCCCTTTCCCTC	766	55
19	GAGTCATGATATGACTATGC	TAAAGGCTATGCTCTATCTC	469	58
20	AAATTCTGTCATTGCCTTTC	GATGTGTGTGAAATAAATGC	330	58

21	TGACAGTCAGTGCTCTTGTCAC	ACCCTTGGCTTACACCTTCA	583	55
22	AAGGCTAAATGTTGTACGAC	CTCTGAGTTATGAGTTACAC	497	58
23	TGAGTTATTCTACCGGCTAATGC	AATGCCTCTGTGGAAAGCTG	453	53
24	GAAATGTATGTGATCATGTC	ACACACACAGGTAAATTTAC	405	49
25	TCTTGAGGCCTTAAAACACC	AGCCCTAGTGATGAGTAAAC	378	57
26	TGGCTATACTAAGTATGGAC	TGCTAGGATACTTTTCTCTC	546	58
27	AGAGCAAGAGAGACCATCTC	TCTCCACTGAAAAGCACATC	419	58
28	ATGTGTTCAGGAGTAGCTAC	ACACGGAGAGCAAAAATCAC	291	58

*base pair

Table 2.3: List of primers used in screening *INPP5E* gene

Exon No.	PRIMER (5′→3′)		Product Size *(bp)	Annealing Temp (°C)
	Forward	**Reverse**		
1-1	CGTTTCTGCTCCTCGCTGC	TCCTGCAAGGAGGTGCTCAG	485	62
1-2	AGCCAGGAGGACCTGGAAGC	GTTCTTTCCGGTTAGGCATC	430	59
2	GCAGCTCCTGACATTCCATG	TTAGCAGTGGGGTGCACCTC	560	60
3	ACAGACTCGTGCTTGGAGAG	CATGACCACAGGTCTCAGCA	545	56
4-5	ATTGCTTCTCCGCGCAAGAC	GCGTGCATCTTAGCAAGCGT	470	57
6	GCACCACGCTTGCTAAGATG	ATTCGCACTGGGACAGTTCC	410	57
7	TTCTGGAACTGTCCCAGTGC	TCTCCTCATCTCCCTCCATG	458	57
8	GAGATGAGGAGAGGTGAGG	CTCAGTGGCTTCTTGAGGCT	380	58
9	GCCTGGACTTGAAACTCAGC	TCTTAGCTCATGGGACGACG	475	58
10	CCACTTGGGGCTTTGTTCTG	CTGTATGGACCTGCCATGGA	415	61

*base pair

RESULTS

RESULTS

Description of the Families Studied

Family A

Family A is located in Haripur district in the NWFP, Pakistan. Traditionally, members of this family prefer to marry within the tribe and consequently consanguineous marriages are common. The six-generation pedigree (Figure 3.1) consists of 44 individuals, including six affected males (V-6, V-7, VI-1, VI-4, VI-7 and VI-10) and six affected females (V-5, V-8, VI-3, VI-5, VI-8 and VI-11). An affected male (VI-4) is deceased. Analysis of pedigree is strongly suggestive of autosomal recessive mode of inheritance and consanguineous loops could account for all the affected persons being homozygous for the abnormal allele. The affected individuals are present in generation fifth and sixth. The parents IV-8 and IV-9; V-1 and V-2; V-3 and V-4 are normal phenotypically, but resulted in 4 (V-5, V-6, V-7 and V-8), 4 (VI-1, VI-3, VI-4 and VI-5) and 4 (VI-7, VI-8, VI-10 and VI-11) affected children, respectively. In all the affected individuals, microcephaly is present by birth. The mental retardation was very mild in the affected individuals. Average head circumferences of affected and normal individuals are 38 cm and 50 cm, respectively. The parents have normal head circumference and intelligence.

Blood samples were collected from 15 individuals including eight affected (V-5, V-6, VI-1, VI-5, VI-7, VI-8, VI-10 and VI-11) and seven normal (V-1, V-3, V-4, VI-2, VI-6, VI-9 and VI-12) individuals of the family. Affected individuals (V-7, V-8 and VI-3) were not available at the time of study. DNA extraction was performed using standard inorganic/organic methods.

Family B

This family with primary microcephaly belongs to district Lahore in the Punjab province of Pakistan. The family members are engaged in regular farming and cattle herding. Owing to strict social customs the family members rarely marry outside the community. Four generation pedigree (Figure 3.3) consists of 14 individuals including three affected males (IV-3, IV-4, and IV-6) and one affected female (IV-2). Pedigree analysis is suggestive of autosomal recessive mode of inheritance and consanguineous loops could account of all the affected persons being homozygous for an abnormal

allele. The parents III-1 and III-2 are normal phenotypically, but resulted in 4 (IV-2, IV-3, IV-4 and IV-6) affected children. Microcephaly is congenital in all the affected individuals. Affected individuals are mild to moderate mentally retarded; otherwise they have no associated abnormality. Average head circumferences of affected and normal individuals are 37 cm and 48 cm, respectively. The facial features of affected individuals are normal. All the carriers have normal phenotype.

DNA was extracted from the blood samples collected from seven family members including three normal (III-1, III-2 and IV-5) and four affected (IV-2, IV-3, IV-4 and IV-6) individuals.

Family C

The family C resides in district Bannu of NWFP, Pakistan. The family members are engaged in small businesses in the local market. The traditional system of marriages within the community results in high rate of consanguineous marriages. The pedigree drawing presented in Figure 3.5 indicates four generations with two affected males (IV-6 and IV-7) and two affected females (IV-1 and IV-3). Affected individuals being produced by the unaffected parents and the affected status was independent of the sex suggesting that the trait is transmitted in autosomal recessive manner. The parents III-1 and III-2, and III-3 and III-4 are normal phenotypically, but resulted in two (IV-1 and IV-3) and two (IV-6 and IV-7) affected individuals, respectively. Microcephaly is congenital in all the affected individuals; affected individuals are mild to moderate mentally retarded, but they have no other associated abnormality. Figure 3.6 shows affected individuals (IV-6 and IV-7) of the family. Average head circumferences of affected and normal individuals are 38.25 cm and 49.5 cm, respectively.

Blood samples were collected from six family members including four affected (IV-1, IV-3, IV-6 and IV-7) and two normal (III-2 and III-3) individuals and DNA extraction was performed using standard inorganic/organic methods.

Family D

This family with primary microcephaly was located in district Kohat of NWFP, Pakistan. The family members traditionally marry within the community due to strict social customs. The family pedigree (Figure 3.7) consists of four generations with four affected individuals (IV-1, IV-2, IV-5 and IV-6). Pedigree analysis is strongly suggestive of autosomal recessive mode of inheritance and consanguineous loops

could account for all the affected persons being homozygous for the abnormal allele. In the pedigree the parents III-1 and III-2, and III-3 and III-4 are normal phenotypically but resulted in two affected (IV-1 and IV-2) and two affected (IV-5 and IV-6) offspring, respectively. Mental retardation is mild to moderate in all the affected individuals but they have learned several self-help skills. The facial features of the affected individuals are normal except an indistinct slopping forehead (Figure 3.8). Average head circumferences of both affected and normal individuals are 37 cm and 46 cm, respectively.

Blood samples were collected from six family members including four normal (III-1, III-3, III-4 and IV-4) and two affected individuals (IV-1 and IV-6). DNA extraction was performed using standard inorganic/organic methods.

Genetic Linkage Studies

On the basis of genetic linkage studies in autosomal recessive primary microcephaly, it is clear that at least some candidate intervals should be tested for linkage or exclusion prior to embarking on genome-wide scan. Eight candidate loci (MCPH 1-8) for autosomal recessive primary microcephaly are known. The linkage of a family to the MCPH locus was based on the observation that all affected individuals had the same homozygous pattern. In case the affected individuals showed a heterozygous marker pattern, the corresponding family was considered as not linked.

In the present study, all the four families were tested for linkage to the known loci by genotyping microsatellite markers mapped within the candidate linkage intervals. Table 2.1 summarizes the microsatellite markers in the region of known loci, which were used in the present study for candidate gene mapping. Average heterozygosity for the selected markers is greater than 70%. Analysis of microsatellite markers was carried out using a standard PCR reaction and electrophoresis in 8% non-denaturing polyacrylamide gel as discussed in Materials and Methods. Amplified PCR products were visualized by staining the gel with ethidium bromide and genotypes were assigned by visual inspection.

In family A, fifteen DNA samples including eight affected (V-5, V-6, VI-1, VI-5, VI-7, VI-8, VI-10 and VI-11) and seven normal (V-1, V-3, V-4, VI-2, VI-6, VI-9 and VI-12) individuals were used for genotyping. DNA analysis with polymorphic microsatellite markers (D1S2625, GATA135FO2, D1S1183, D1S1660,) linked to

MCPH5 candidate linkage interval (Figures 3.9-3.12) revealed that all the affected individuals were homozygous while normal were heterozygous, thus establishing linkage of family A to MCPH5 locus on chromosome 1q31-32.

Genotyping of seven members of the family B including three normal (III-1, III-2 and IV-5) and four affected (IV-2, IV-3, IV-4 and IV-6) individuals, was carried out by using polymorphic microsatellite markers D1S2625, D1S2816, D1S1660, D1S2716, which are closely linked to the MCPH5 locus. The markers were fully informative (Figures 3.13-3.16) and all the affected members of the family were homozygous for these four markers, suggesting linkage to the MCPH5 locus on chromosome 1q31-32.

In family C, six DNA samples including four affected (IV-1, IV-3, IV-6 and IV-7) and two normal (III-2 and III-3) individuals were used for genotyping. DNA analysis with polymorphic microsatellite markers (D1S3468, D1S2625, D1S408, D1S1660) linked to MCPH5 candidate linkage interval (Figures 3.17-3.20) revealed that these markers were homozygous in all the affected individuals but heterozygous in normal individuals, thus establishing linkage of family C to MCPH5 locus on chromosome 1q31-32.

Family D

The family D was tested for linkage by using microsatellite markers tightly linked to seven candidate loci (MCPH1-MCPH7) for autosomal recessive primary microcephaly (Table 2.1). These included: MCPH1 locus at 8p22-pter, MCPH2 locus at 19q13.1-13.2, MCPH3 locus at 9q34, MCPH4 locus at 15q15-21, MCPH5 locus at 1q25-32, MCPH6 locus at 13q12.2 and MCPH7 locus at 9q34.3. Analysis of the results obtained by genotyping polymorphic microsatellite markers (Figures 3.21-3.44) excluded the family from linkage to the six loci (MCPH1-MCPH6). DNA analysis with polymorphic microsatellite markers (D9S1818, D9S1826, D9S158, D9S905) linked to MCPH7 candidate linkage interval (Figures 3.45-3.48) revealed that three markers (D9S1818, D9S1826, D9S158) were homozygous in all the affected individuals but heterozygous in normal individuals, thus establishing linkage of family D to MCPH7 locus on chromosome 9q34.3.

Sequencing *ASPM* Gene at MCPH5

Genotyping analysis showed linkage of these families (A, B and C) to MCPH5 locus harboring *ASPM* gene. Therefore, *ASPM* gene was sequenced in affected and normal individuals of these three families. Primers to amplify 28 exons (Table 2.2) were designed from the intron- exon boundary sequences of the *ASPM* gene (Gul *et al.*, 2006).

In families A and B, the entire coding region and splice junctions of *ASPM* gene were screened in two affected and one normal individual of the families. Human sequence analysis failed to detect pathogenic sequence variant suggesting that probably the mutations are present in regulatory sequences of the gene.

In family C sequence analysis showed a previously characterized nonsense mutation 3978 G > A (W1326 X) (Kumar *et al.*, 2004) in exon 17 of the *ASPM* gene (Figure 3.45). All the affected were homozygous and the carriers were heterozygous for this mutation. The mutation resulted in changing codon TGG for amino acid Tryptophane to TGA the stop codon and resulted in immediate stop of translation and in turn caused protein truncation and thus pathogenesis.

Sequencing *INPP5E* Gene at MCPH7

Genotyping analysis showed linkage of family D to MCPH7 locus harboring *INPP5E* gene. Therefore, *INPP5E* gene was sequenced in two affected and one normal individuals of the family. Primers to amplify 10 exons (Table 2.3) of this gene were designed from the intron- exon boundary sequences of the gene. Sequence analysis of the entire coding region and splice junctions of *INPP5E* gene failed to detect pathogenic sequence variant suggesting that the mutation is probably present in the regulatory sequences of the gene.

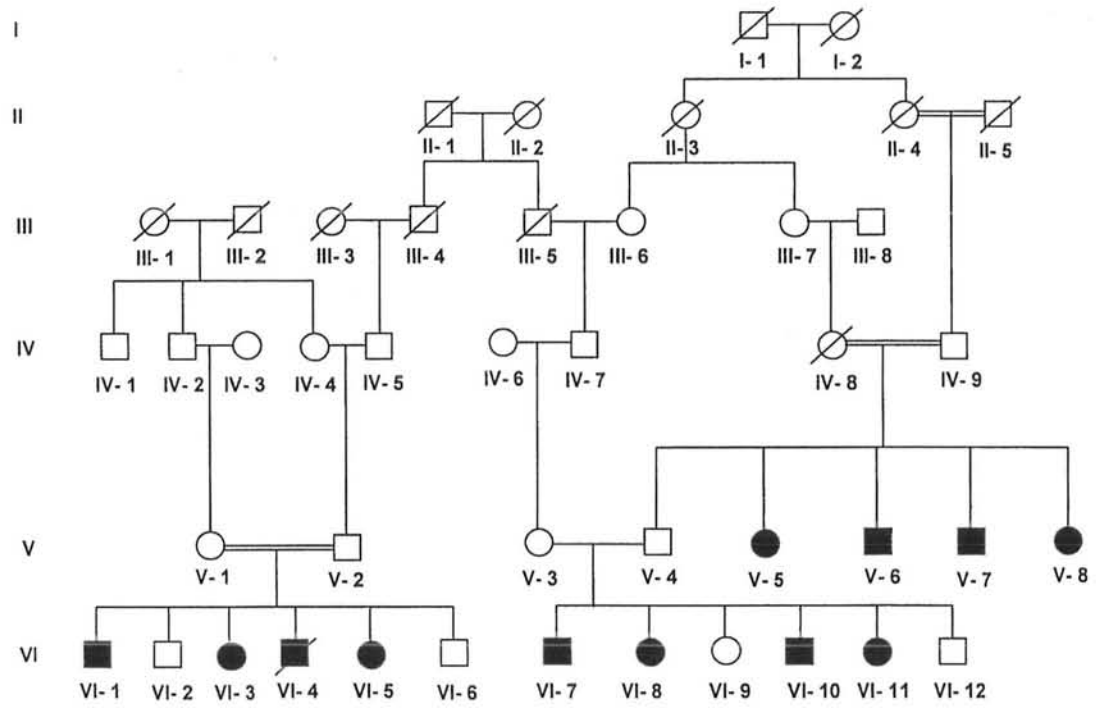

Figure 3.1: Pedigree of family A with primary microcephaly. Circles represent females and squares represent males. Filled circles and squares represent affected individuals. Double lines indicate consanguineous marriages. Cross lines on the symbols represent deceased individuals.

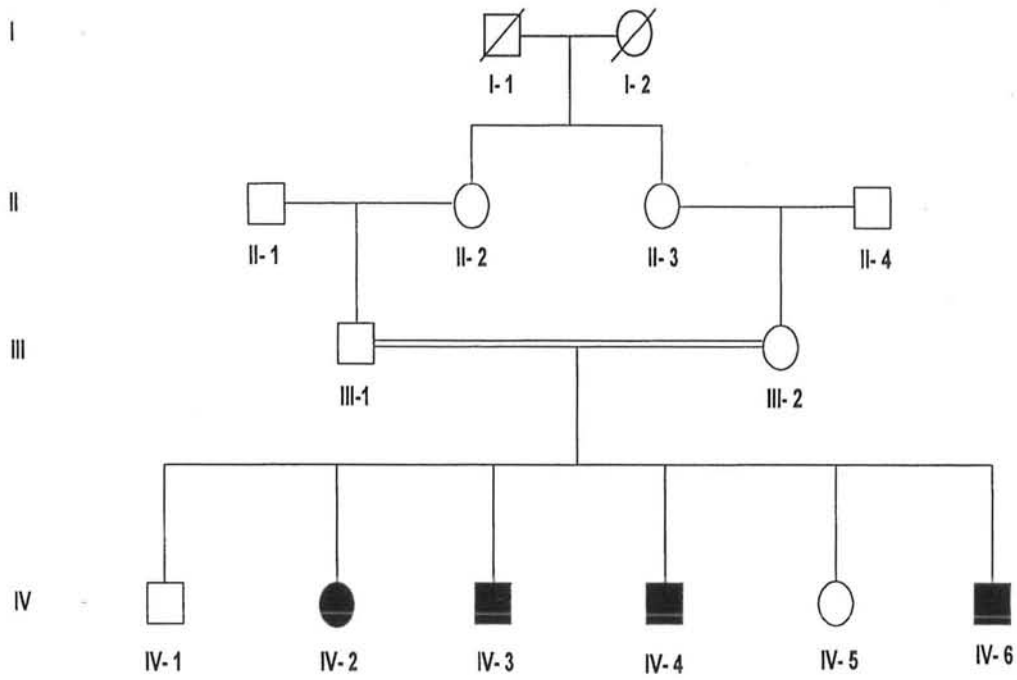

Figure 3.2: Pedigree of family B with primary microcephaly. Circles represent females and squares represent males. Filled circles and squares represent affected individuals. Double lines indicate consanguineous marriages. Cross lines on the symbols represent deceased individuals.

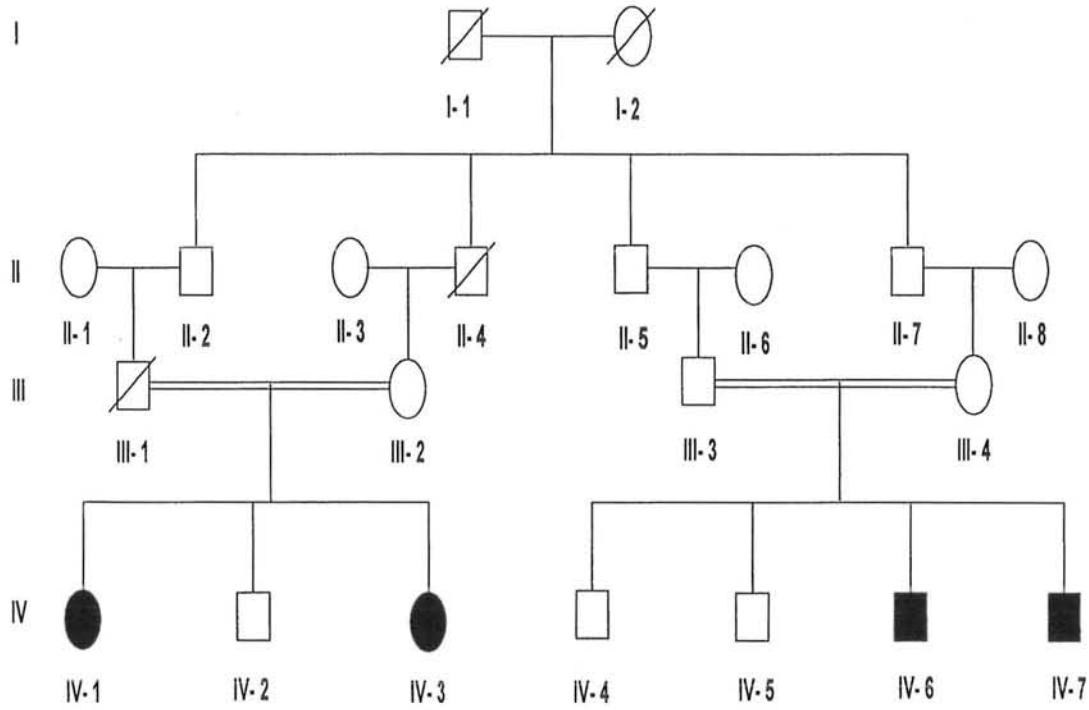

Figure 3.3: Pedigree of family C with primary microcephaly. Circles represent females and squares represent males. Filled circles and squares represent affected individuals. Double lines indicate consanguineous marriages. Cross lines on the symbols represent deceased individuals.

a

b

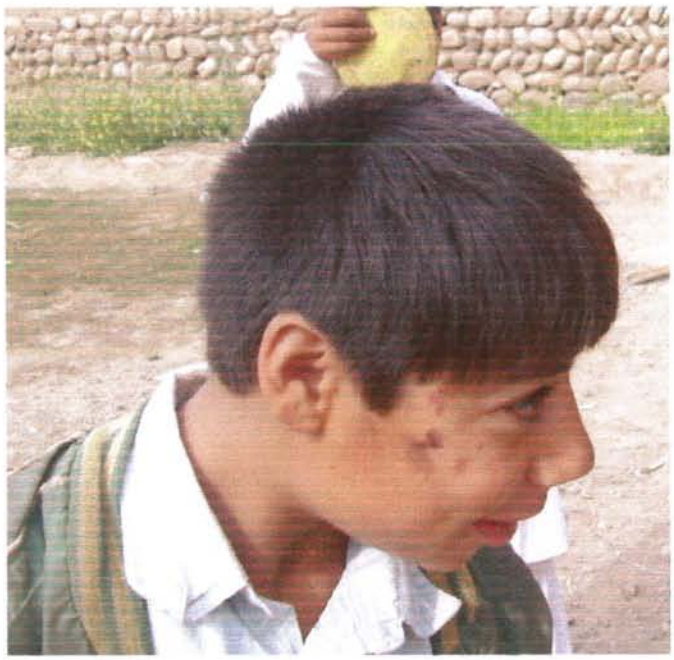

Figure 3.4: Clinical photographs representing the affected siblings IV-6 (a) and IV-7 (b) of family C with autosomal recessive primary microcephaly.

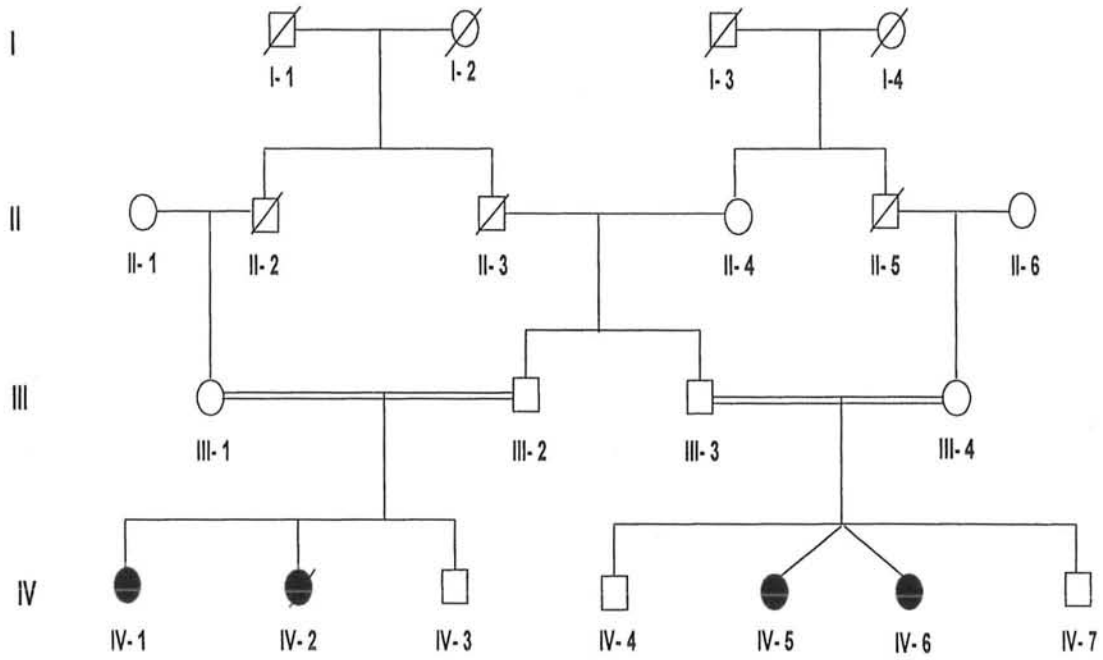

Figure 3.5: Pedigree of family D with primary microcephaly. Circles represent females and squares represent males. Filled circles and squares represent affected individuals. Double lines indicate consanguineous marriages. Cross lines on the symbols represent deceased individuals.

a

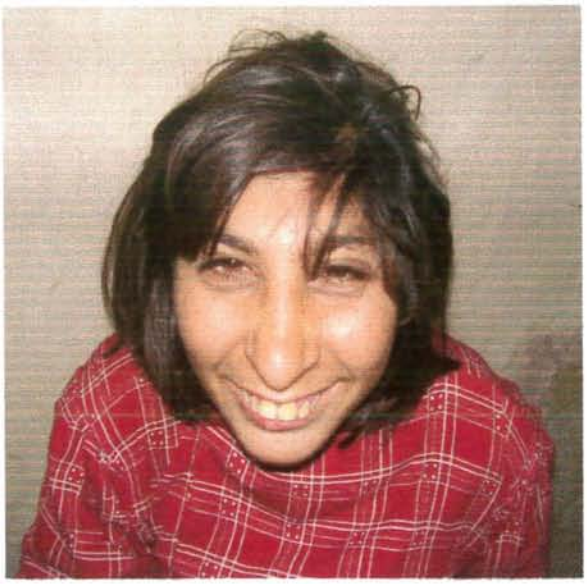

b

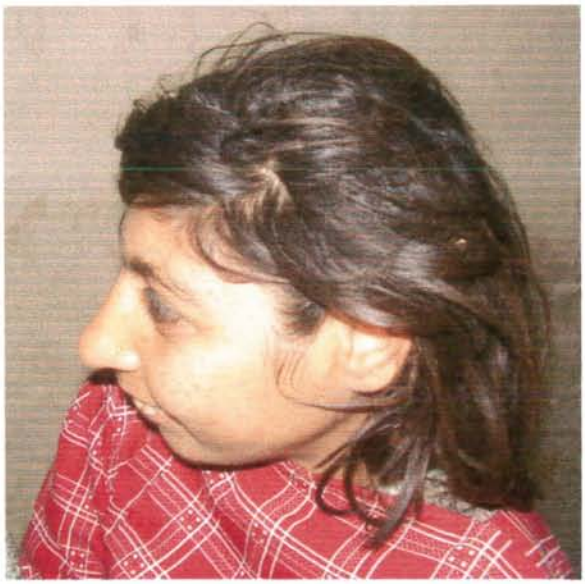

Figure 3.6: Clinical picture representing the affected individuals IV-1 (a) and IV-6 (b) of Family D with primary autosomal recessive primary microcephaly.

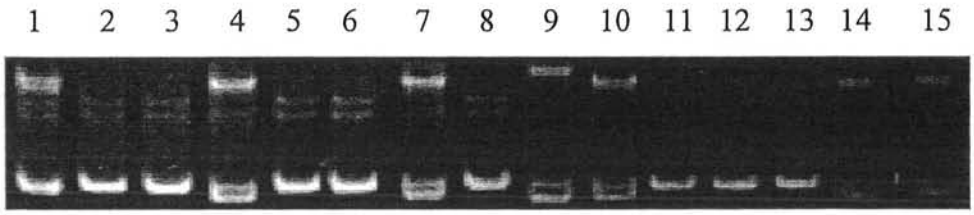

Family A

Lane 1.	V-1	Normal	Lane 6.	VI-5	Affected	Lane 11.	VI-8	Affected
Lane 2.	V-5	Affected	Lane 7.	VI-6	Normal	Lane 12.	VI-10	Affected
Lane 3.	V-6	Affected	Lane 8.	VI-7	Affected	Lane 13.	VI-11	Affected
Lane 4.	VI-2	Normal	Lane 9.	V-3	Normal	Lane 14.	VI-9	Normal
Lane 5.	VI-1	Affected	Lane 10.	V-4	Normal	Lane 15.	VI-12	Affected

Figure 3.7: Electropherogram of ethidium bromide stained 8% non-denaturing polyacrylamide gel for marker D1S2625 at 208.26 cM from MCPH5 candidate linkage interval at 1q31 showing homozygosity in the affected individuals (V-5, V-6, VI-1, VI-5, VI-7, VI-8, VI-10, VI-11) of family A. The Roman numerals indicate the generation number of the individuals within a pedigree while Arabic numerals indicate their positions within generation.

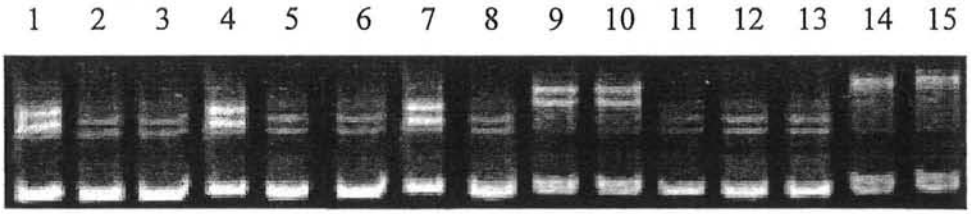

Family A

Lane 1.	V-1	Normal	Lane 6.	VI-5	Affected	Lane 11.	VI-8	Affected
Lane 2.	V-5	Affected	Lane 7.	VI-6	Normal	Lane 12.	VI-10	Affected
Lane 3.	V-6	Affected	Lane 8.	VI-7	Affected	Lane 13.	VI-11	Affected
Lane 4.	VI-2	Normal	Lane 9.	V-3	Normal	Lane 14.	VI-9	Normal
Lane 5.	VI-1	Affected	Lane 10.	V-4	Normal	Lane 15.	VI-12	Affected

Figure 3.8: Electropherogram of ethidium bromide stained 8% non-denaturing polyacrylamide gel for marker GATA135FO2 at 211.73 cM from MCPH5 candidate linkage interval at 1q31 showing homozygosity in the affected individuals (V-5, V-6, VI-1, VI-5, VI-7, VI-8, VI-10, VI-11) of family A. The Roman numerals indicate the generation number of the individuals within a pedigree while Arabic numerals indicate their positions within generation.

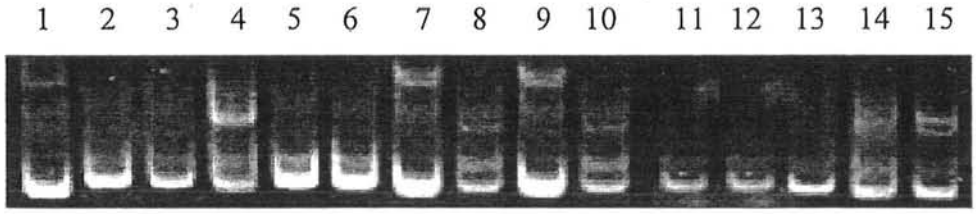

Family A

Lane 1.	V-1	Normal	Lane 6.	VI-5	Affected	Lane 11.	VI-8	Affected
Lane 2.	V-5	Affected	Lane 7.	VI-6	Normal	Lane 12.	VI-10	Affected
Lane 3.	V-6	Affected	Lane 8.	VI-7	Affected	Lane 13.	VI-11	Affected
Lane 4.	VI-2	Normal	Lane 9.	V-3	Normal	Lane 14.	VI-9	Normal
Lane 5.	VI-1	Affected	Lane 10.	V-4	Normal	Lane 15.	VI-12	Affected

Figure 3.9: Electropherogram of ethidium bromide stained 8% non-denaturing polyacrylamide gel for marker D1S1183 at 211.89 cM from MCPH5 candidate linkage interval at 1q31 showing homozygosity in the affected individuals (V-5, V-6, VI-1, VI-5, VI-7, VI-8, VI-10, VI-11) and normal individuals (V-4, VI-9) of family A. The Roman numerals indicate the generation number of the individuals within a pedigree while Arabic numerals indicate their positions within generation.

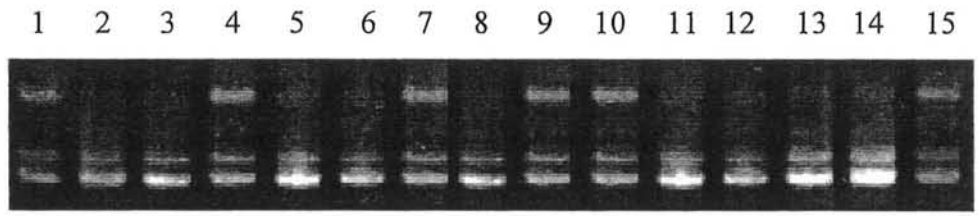

Family A

Lane 1.	V-1	Normal	Lane 6.	VI-5	Affected	Lane 11.	VI-8	Affected
Lane 2.	V-5	Affected	Lane 7.	VI-6	Normal	Lane 12.	VI-10	Affected
Lane 3.	V-6	Affected	Lane 8.	VI-7	Affected	Lane 13.	VI-11	Affected
Lane 4.	VI-2	Normal	Lane 9.	V-3	Normal	Lane 14.	VI-9	Normal
Lane 5.	VI-1	Affected	Lane 10.	V-4	Normal	Lane 15.	VI-12	Affected

Figure 3.10: Electropherogram of ethidium bromide stained 8% non-denaturing polyacrylamide gel for marker D1S1660 at 213.11 cM from MCPH5 candidate linkage interval at 1q31 showing homozygosity in the affected individual (V-5, V-6, VI-1, VI-5, VI-7, VI-8, VI-10, VI-11) and normal individual (VI-9) of family A. The Roman numerals indicate the generation number of the individuals within a pedigree while Arabic numerals indicate their positions within generation

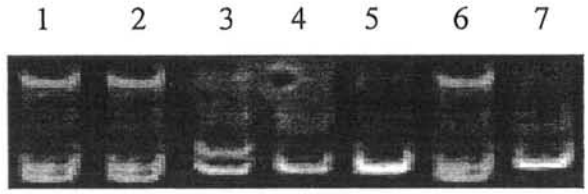

Family B

Lane 1.	III-1	Normal	Lane 5.	IV-4	Affected
Lane 2.	III-2	Normal	Lane 6.	IV-5	Normal
Lane 3.	IV-2	Affected	Lane 7.	IV-6	Affected
Lane 4.	IV-3	Affected			

Figure 3.11: Electropherogram of ethidium bromide stained 8% non-denaturing polyacrylamide gel for marker D1S2625 at 208.26 cM from MCPH5 candidate linkage interval at 1q31 showing homozygosity in the affected individuals (IV-2, IV-3, IV-4, IV-6) of family B. The Roman numerals indicate the generation number of the individuals within a pedigree while Arabic numerals indicate their positions within generation.

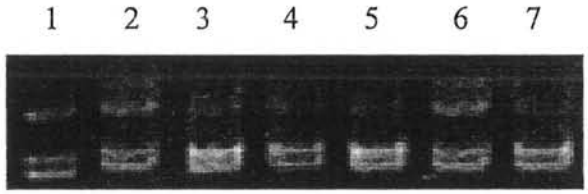

Family B

Lane 1.	III-1	Normal	Lane 5.	IV-4	Affected
Lane 2.	III-2	Normal	Lane 6.	IV-5	Normal
Lane 3.	IV-2	Affected	Lane 7.	IV-6	Affected
Lane 4.	IV-3	Affected			

Figure 3.12: Electropherogram of ethidium bromide stained 8% non-denaturing polyacrylamide gel for marker D1S2816 at 211.89 cM from MCPH5 candidate linkage interval at 1q31 showing homozygosity in the affected individuals (IV-2, IV-3, IV-4, IV-6) of family B. The Roman numerals indicate the generation number of the individuals within a pedigree while Arabic numerals indicate their positions within generation

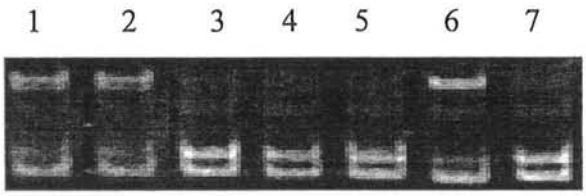

Family B

Lane 1.	III-1	Normal	Lane 5.	IV-4	Affected
Lane 2.	III-2	Normal	Lane 6.	IV-5	Normal
Lane 3.	IV-2	Affected	Lane 7.	IV-6	Affected
Lane 4.	IV-3	Affected			

Figure 3.13: Electropherogram of ethidium bromide stained 8% non-denaturing polyacrylamide gel for marker D1S1660 at 213.11 cM from MCPH5 candidate linkage interval at 1q31 showing homozygosity in the affected individuals (IV-2, IV-3, IV-4, IV-6) of family B. The Roman numerals indicate the generation number of the individuals within a pedigree while Arabic numerals indicate their positions within generation

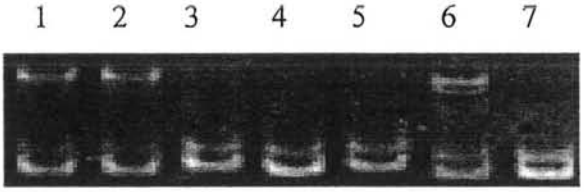

Family B

Lane 1.	III-1	Normal	Lane 5.	IV-4	Affected
Lane 2.	III-2	Normal	Lane 6.	IV-5	Normal
Lane 3.	IV-2	Affected	Lane 7.	IV-6	Affected
Lane 4.	IV-3	Affected			

Figure 3.14: Electropherogram of ethidium bromide stained 8% non-denaturing polyacrylamide gel for marker D1S2716 at 215.44 cM from MCPH5 candidate linkage interval at 1q31 showing homozygosity in the affected individuals (IV-2, IV-3, IV-4, IV-6) of family B. The Roman numerals indicate the generation number of the individuals within a pedigree while Arabic numerals indicate their positions within generation

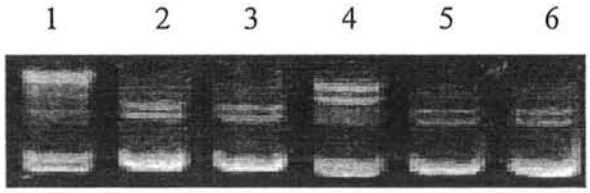

Family C

Lane 1.	III-2	Normal	Lane 4.	III-3	Normal
Lane 2.	IV-1	Affected	Lane 5.	IV-6	Affected
Lane 3.	IV-3	Affected	Lane 6.	IV-7	Affected

Figure 3.15 Electropherogram of ethidium bromide stained 8% non-denaturing polyacrylamide gel for marker D1S3468 at 205.4 cM from MCPH5 candidate linkage interval at 1q31 showing homozygosity in the affected individuals (IV-1, IV-3, IV-6, IV-7) of family C. The Roman numerals indicate the generation number of the individuals within a pedigree while Arabic numerals indicate their positions within generation

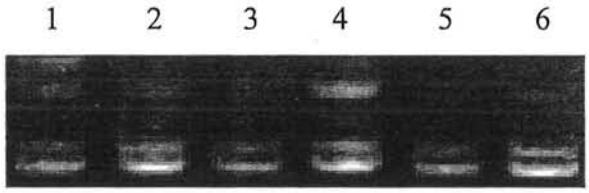

Family C

Lane 1.	III-2	Normal	Lane 4.	III-3	Normal
Lane 2.	IV-1	Affected	Lane 5.	IV-6	Affected
Lane 3.	IV-3	Affected	Lane 6.	IV-7	Affected

Figure 3.16: Electropherogram of ethidium bromide stained 8% non-denaturing polyacrylamide gel for marker D1S2625 at 208.26 cM from MCPH5 candidate linkage interval at 1q31 showing homozygosity in the affected individuals (IV-1, IV-3, IV-6, IV-7) of family C. The Roman numerals indicate the generation number of the individuals within a pedigree while Arabic numerals indicate their positions within generation

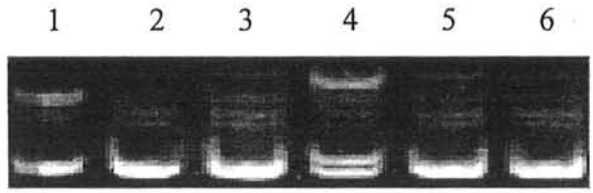

Family C

Lane 1.	III-2	Normal	Lane 4.	III-3	Normal
Lane 2.	IV-1	Affected	Lane 5.	IV-6	Affected
Lane 3.	IV-3	Affected	Lane 6.	IV-7	Affected

Figure 3.17: Electropherogram of ethidium bromide stained 8% non-denaturing polyacrylamide gel for marker D1S408 at 210.78 cM from MCPH5 candidate linkage interval at 1q31 showing homozygosity in the affected individuals (IV-1, IV-3, IV-6, IV-7) of family C. The Roman numerals indicate the generation number of the individuals within a pedigree while Arabic numerals indicate their positions within generation

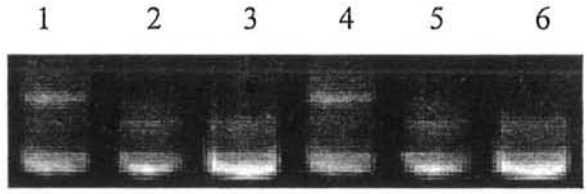

Family C

Lane 1.	III-2	Normal	Lane 4.	III-3	Normal
Lane 2.	IV-1	Affected	Lane 5.	IV-6	Affected
Lane 3.	IV-3	Affected	Lane 6.	IV-7	Affected

Figure 3.18: Electropherogram of ethidium bromide stained 8% non-denaturing polyacrylamide gel for marker D1S1660 at 213.11 cM from MCPH5 candidate linkage interval at 1q31 showing homozygosity in the affected individuals (IV-1, IV-3, IV-6, IV-7) of family C. The Roman numerals indicate the generation number of the individuals within a pedigree while Arabic numerals indicate their positions within generation

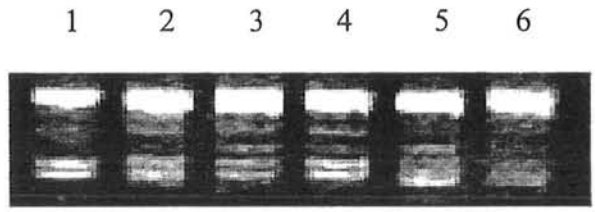

Family D

Lane 1.	IV-1	Affected	Lane 4.	III-1	Normal
Lane 2.	IV-6	Affected	Lane 5.	III-3	Normal
Lane 3.	III-4	Normal	Lane 6.	IV-4	Normal

Figure 3.19: Electropherogram of ethidium bromide stained 8% non-denaturing polyacrylamide gel for marker D8S518 at 9.88 cM from MCPH1 candidate linkage interval on chromosome 8p22-pter, of family D. The Roman numerals indicate the generation number of the individuals within a pedigree while Arabic numerals indicate their positions within generation.

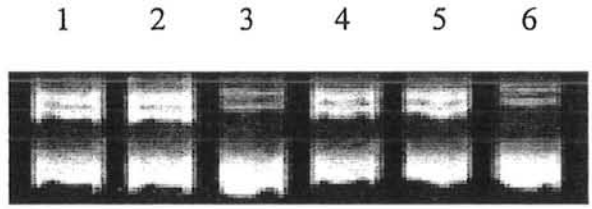

Family D

Lane 1.	IV-1	Affected	Lane 4.	III-1	Normal
Lane 2.	IV-6	Affected	Lane 5.	III-3	Normal
Lane 3.	III-4	Normal	Lane 6.	IV-4	Normal

Figure 3.20: Electropherogram of ethidium bromide stained 8% non-denaturing polyacrylamide gel for marker D8S1798 at 11.96 cM from MCPH1 candidate linkage interval on chromosome 8p22-pter, of family D. The Roman numerals indicate the generation number of the individuals within a pedigree while Arabic numerals indicate their positions within generation.

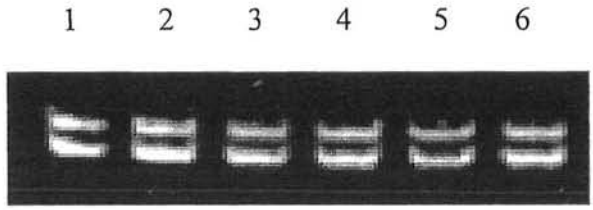

Family D

Lane 1.	IV-1	Affected	Lane 4.	III-1	Normal
Lane 2.	IV-6	Affected	Lane 5.	III-3	Normal
Lane 3.	III-4	Normal	Lane 6.	IV-4	Normal

Figure 3.21: Electropherogram of ethidium bromide stained 8% non-denaturing polyacrylamide gel for marker D8S1742 at 13.72 cM from MCPH1 candidate linkage interval on chromosome 8p22-pter, of family D. The Roman numerals indicate the generation number of the individuals within a pedigree while Arabic numerals indicate their positions within generation.

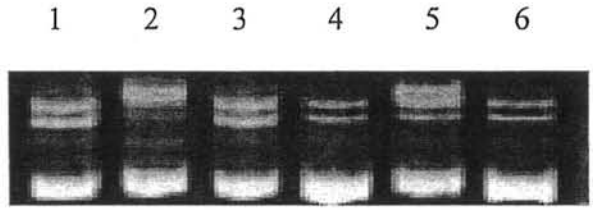

Family D

Lane 1.	IV-1	Affected	Lane 4.	III-1	Normal
Lane 2.	IV-6	Affected	Lane 5.	III-3	Normal
Lane 3.	III-4	Normal	Lane 6.	IV-4	Normal

Figure 3.22: Electropherogram of ethidium bromide stained 8% non-denaturing polyacrylamide gel for marker D8S561 at 15.04 cM from MCPH1 candidate linkage interval on chromosome 8p22-pter, of family D. The Roman numerals indicate the generation number of the individuals within a pedigree while Arabic numerals indicate their positions within generation.

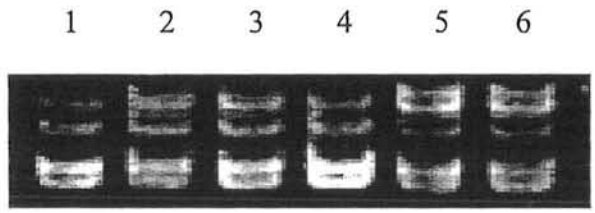

Family D

Lane 1.	IV-1	Affected	Lane 4.	III-1	Normal
Lane 2.	IV-6	Affected	Lane 5.	III-3	Normal
Lane 3.	III-4	Normal	Lane 6.	IV-4	Normal

Figure 3.23: Electropherogram of ethidium bromide stained 8% non-denaturing polyacrylamide gel for marker D19S416 at 56.28 cM from MCPH2 candidate linkage interval on chromosome 19q13-13.2, of family D. The Roman numerals indicate the generation number of the individuals within a pedigree while Arabic numerals indicate their positions within generation.

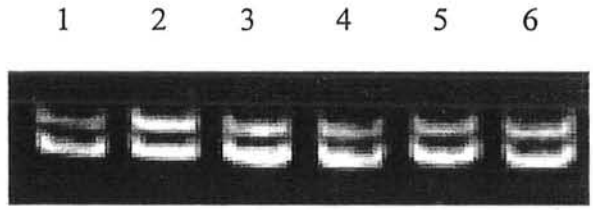

Family D

Lane 1.	IV-1	Affected	Lane 4.	III-1	Normal
Lane 2.	IV-6	Affected	Lane 5.	III-3	Normal
Lane 3.	III-4	Normal	Lane 6.	IV-4	Normal

Figure 3.24: Electropherogram of ethidium bromide stained 8% non-denaturing polyacrylamide gel for marker D19S220 at 62.62 cM from MCPH2 candidate linkage interval on chromosome 19q13-13.2, of family D. The Roman numerals indicate the generation number of the individuals within a pedigree while Arabic numerals indicate their positions within generation.

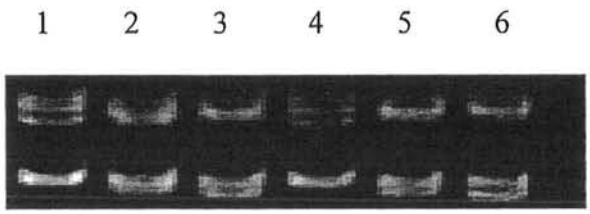

Family D

Lane 1.	IV-1	Affected	Lane 4.	III-1	Normal
Lane 2.	IV-6	Affected	Lane 5.	III-3	Normal
Lane 3.	III-4	Normal	Lane 6.	IV-4	Normal

Figure 3.25: Electropherogram of ethidium bromide stained 8% non-denaturing polyacrylamide gel for marker D19S223 at 66.09 cM from MCPH2 candidate linkage interval on chromosome 19q13-13.2, of family D. The Roman numerals indicate the generation number of the individuals within a pedigree while Arabic numerals indicate their positions within generation.

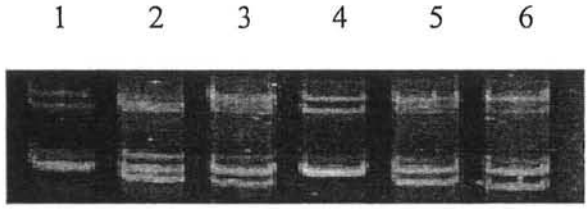

Family D

Lane 1.	IV-1	Affected	Lane 4.	III-1	Normal
Lane 2.	IV-6	Affected	Lane 5.	III-3	Normal
Lane 3.	III-4	Normal	Lane 6.	IV-4	Normal

Figure 3.26: Electropherogram of ethidium bromide stained 8% non-denaturing polyacrylamide gel for marker D19S197 at 67.72 cM from MCPH2 candidate linkage interval on chromosome 19q13-13.2, of family D. The Roman numerals indicate the generation number of the individuals within a pedigree while Arabic numerals indicate their positions within generation.

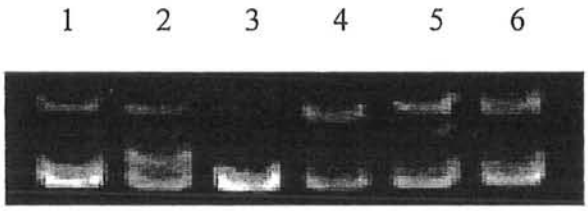

Family D

Lane 1.	IV-1	Affected	Lane 4.	III-1	Normal
Lane 2.	IV-6	Affected	Lane 5.	III-3	Normal
Lane 3.	III-4	Normal	Lane 6.	IV-4	Normal

Figure 3.27: Electropherogram of ethidium bromide stained 8% non-denaturing polyacrylamide gel for marker D9S1776 at 123.79 cM from MCPH3 candidate linkage interval on chromosome 9q34, of family D. The Roman numerals indicate the generation number of the individuals within a pedigree while Arabic numerals indicate their positions within generation.

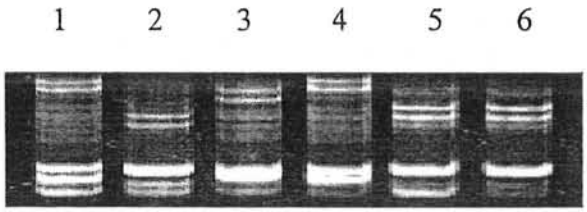

Family D

Lane 1.	IV-1	Affected	Lane 4.	III-1	Normal
Lane 2.	IV-6	Affected	Lane 5.	III-3	Normal
Lane 3.	III-4	Normal	Lane 6.	IV-4	Normal

Figure 3.28: Electropherogram of ethidium bromide stained 8% non-denaturing polyacrylamide gel for marker D9S1872 at 128.65 cM from MCPH3 candidate linkage interval on chromosome 9q34, of family D. The Roman numerals indicate the generation number of the individuals within a pedigree while Arabic numerals indicate their positions within generation.

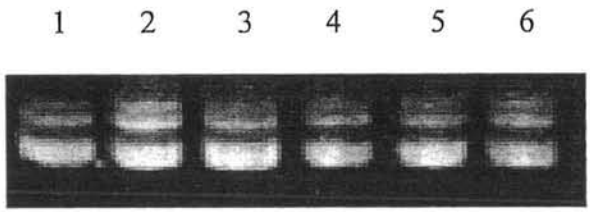

Family D

Lane 1.	IV-1	Affected	Lane 4.	III-1	Normal
Lane 2.	IV-6	Affected	Lane 5.	III-3	Normal
Lane 3.	III-4	Normal	Lane 6.	IV-4	Normal

Figure 3.29: Electropherogram of ethidium bromide stained 8% non-denaturing polyacrylamide gel for marker D9S1850 at 131.56 cM from MCPH3 candidate linkage interval on chromosome 9q34, of family D. The Roman numerals indicate the generation number of the individuals within a pedigree while Arabic numerals indicate their positions within generation.

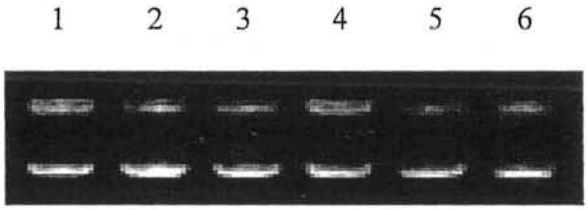

Family D

Lane 1.	IV-1	Affected	Lane 4.	III-1	Normal
Lane 2.	IV-6	Affected	Lane 5.	III-3	Normal
Lane 3.	III-4	Normal	Lane 6.	IV-4	Normal

Figure 3.30: Electropherogram of ethidium bromide stained 8% non-denaturing polyacrylamide gel for marker D9S1881 at 135.52 cM from MCPH3 candidate linkage interval on chromosome 9q34, of family D. The Roman numerals indicate the generation number of the individuals within a pedigree while Arabic numerals indicate their positions within generation.

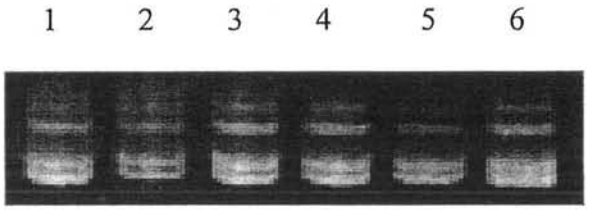

Family D

Lane 1.	IV-1	Affected	Lane 4.	III-1	Normal
Lane 2.	IV-6	Affected	Lane 5.	III-3	Normal
Lane 3.	III-4	Normal	Lane 6.	IV-4	Normal

Figure 3.31 Electropherogram of ethidium bromide stained 8% non-denaturing polyacrylamide gel for marker D15S118 at 32.39 cM from MCPH4 candidate linkage interval on chromosome 15q15-21, of family D. The Roman numerals indicate the generation number of the individuals within a pedigree while Arabic numerals indicate their positions within generation.

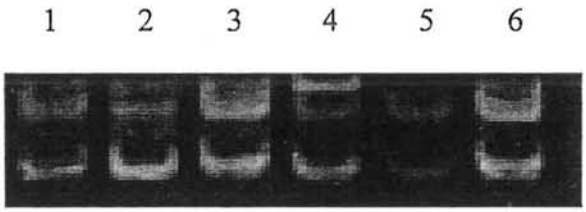

Family D

Lane 1.	IV-1	Affected	Lane 4.	III-1	Normal
Lane 2.	IV-6	Affected	Lane 5.	III-3	Normal
Lane 3.	III-4	Normal	Lane 6.	IV-4	Normal

Figure 3.32: Electropherogram of ethidium bromide stained 8% non-denaturing polyacrylamide gel for marker D15S641 at 41.37 cM from MCPH4 candidate linkage interval on chromosome 15q15-21, of family D. The Roman numerals indicate the generation number of the individuals within a pedigree while Arabic numerals indicate their positions within generation.

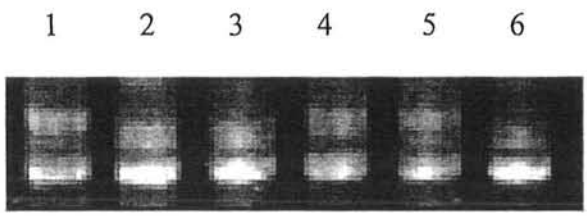

Family D

Lane 1.	IV-1	Affected	Lane 4.	III-1	Normal
Lane 2.	IV-6	Affected	Lane 5.	III-3	Normal
Lane 3.	III-4	Normal	Lane 6.	IV-4	Normal

Figure 3.33: Electropherogram of ethidium bromide stained 8% non-denaturing polyacrylamide gel for marker D15S126 at 47.92 cM from MCPH4 candidate linkage interval on chromosome 15q15-21, of family D. The Roman numerals indicate the generation number of the individuals within a pedigree while Arabic numerals indicate their positions within generation.

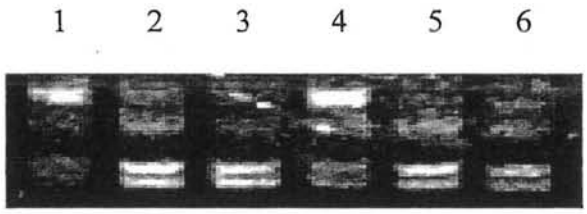

Family D

Lane 1.	IV-1	Affected	Lane 4.	III-1	Normal
Lane 2.	IV-6	Affected	Lane 5.	III-3	Normal
Lane 3.	III-4	Normal	Lane 6.	IV-4	Normal

Figure 3.34: Electropherogram of ethidium bromide stained 8% non-denaturing polyacrylamide gel for marker D15S117 at 55.04 cM from MCPH4 candidate linkage interval on chromosome 15q15-21, of family D. The Roman numerals indicate the generation number of the individuals within a pedigree while Arabic numerals indicate their positions within generation.

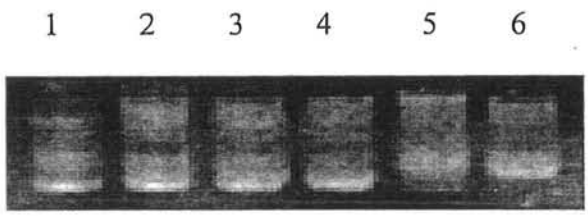

Family D

Lane 1.	IV-1	Affected	Lane 4.	III-1	Normal
Lane 2.	IV-6	Affected	Lane 5.	III-3	Normal
Lane 3.	III-4	Normal	Lane 6.	IV-4	Normal

Figure 3.35: Electropherogram of ethidium bromide stained 8% non-denaturing polyacrylamide gel for marker D1S518 at 205.55 cM from MCPH5 candidate linkage interval on chromosome 1q25-32, of family D. The Roman numerals indicate the generation number of the individuals within a pedigree while Arabic numerals indicate their positions within generation.

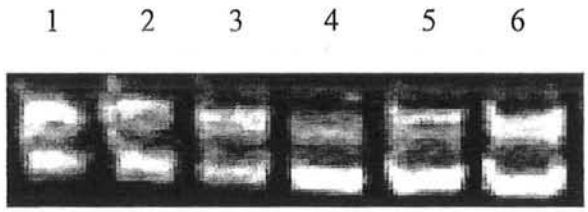

Family D

Lane 1.	IV-1	Affected	Lane 4.	III-1	Normal
Lane 2.	IV-6	Affected	Lane 5.	III-3	Normal
Lane 3.	III-4	Normal	Lane 6.	IV-4	Normal

Figure 3.36: Electropherogram of ethidium bromide stained 8% non-denaturing polyacrylamide gel for marker D1S2823 at 207.86 cM from MCPH5 candidate linkage interval on chromosome 1q25-32, of family D. The Roman numerals indicate the generation number of the individuals within a pedigree while Arabic numerals indicate their positions within generation.

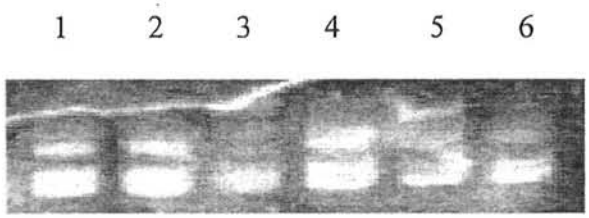

Family D

Lane 1.	IV-1	Affected	Lane 4.	III-1	Normal
Lane 2.	IV-6	Affected	Lane 5.	III-3	Normal
Lane 3.	III-4	Normal	Lane 6.	IV-4	Normal

Figure 3.37: Electropherogram of ethidium bromide stained 8% non-denaturing polyacrylamide gel for marker D1SGATA135FO at 211.73 cM from MCPH5 candidate linkage interval on chromosome 1q25-32, of family D. The Roman numerals indicate the generation number of the individuals within a pedigree while Arabic numerals indicate their positions within generation.

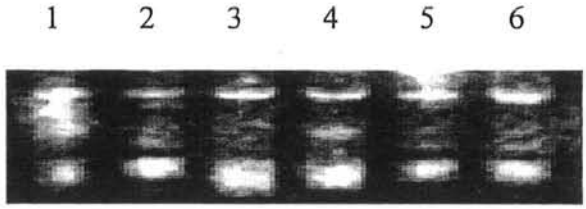

Family D

Lane 1.	IV-1	Affected	Lane 4.	III-1	Normal
Lane 2.	IV-6	Affected	Lane 5.	III-3	Normal
Lane 3.	III-4	Normal	Lane 6.	IV-4	Normal

Figure 3.38: Electropherogram of ethidium bromide stained 8% non-denaturing polyacrylamide gel for marker D1S1726 at 213.8 cM from MCPH5 candidate linkage interval on chromosome 1q25-32, of family D. The Roman numerals indicate the generation number of the individuals within a pedigree while Arabic numerals indicate their positions within generation.

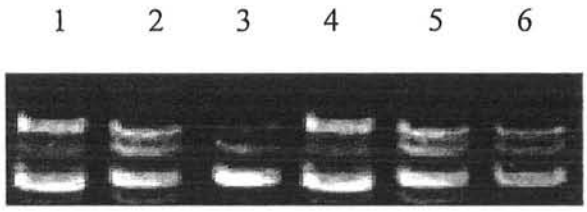

Family D

Lane 1.	IV-1	Affected	Lane 4.	III-1	Normal
Lane 2.	IV-6	Affected	Lane 5.	III-3	Normal
Lane 3.	III-4	Normal	Lane 6.	IV-4	Normal

Figure 3.39: Electropherogram of ethidium bromide stained 8% non-denaturing polyacrylamide gel for marker D13S787 at 8.75 cM from MCPH6 candidate linkage interval on chromosome 13q12.2, of family D. The Roman numerals indicate the generation number of the individuals within a pedigree while Arabic numerals indicate their positions within generation.

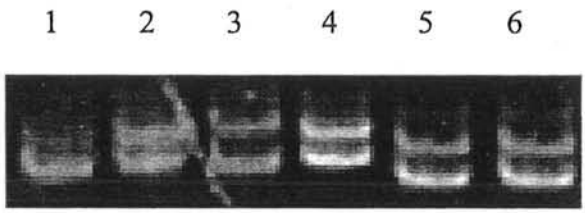

Family D

Lane 1.	IV-1	Affected	Lane 4.	III-1	Normal
Lane 2.	IV-6	Affected	Lane 5.	III-3	Normal
Lane 3.	III-4	Normal	Lane 6.	IV-4	Normal

Figure 3.40: Electropherogram of ethidium bromide stained 8% non-denaturing polyacrylamide gel for marker D13S742 at 11.71 cM from MCPH6 candidate linkage interval on chromosome 13q12.2, of family D. The Roman numerals indicate the generation number of the individuals within a pedigree while Arabic numerals indicate their positions within generation.

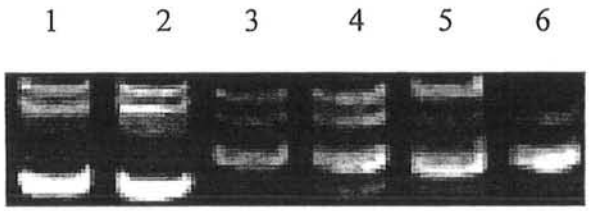

Family D

Lane 1.	IV-1	Affected	Lane 4.	III-1	Normal
Lane 2.	IV-6	Affected	Lane 5.	III-3	Normal
Lane 3.	III-4	Normal	Lane 6.	IV-4	Normal

Figure 3.41: Electropherogram of ethidium bromide stained 8% non-denaturing polyacrylamide gel for marker D13S1294 at 13.94 cM from MCPH6 candidate linkage interval on chromosome 13q12.2, of family D. The Roman numerals indicate the generation number of the individuals within a pedigree while Arabic numerals indicate their positions within generation.

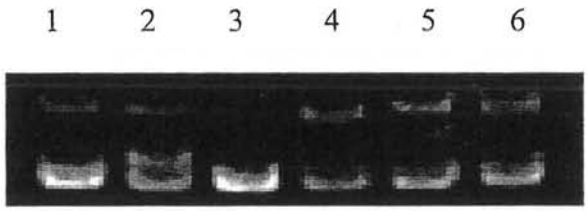

Family D

Lane 1.	IV-1	Affected	Lane 4.	III-1	Normal
Lane 2.	IV-6	Affected	Lane 5.	III-3	Normal
Lane 3.	III-4	Normal	Lane 6.	IV-4	Normal

Figure 3.42: Electropherogram of ethidium bromide stained 8% non-denaturing polyacrylamide gel for marker D13S1304 at 16.05 cM from MCPH6 candidate linkage interval on chromosome 13q12.2, of family D. The Roman numerals indicate the generation number of the individuals within a pedigree while Arabic numerals indicate their positions within generation.

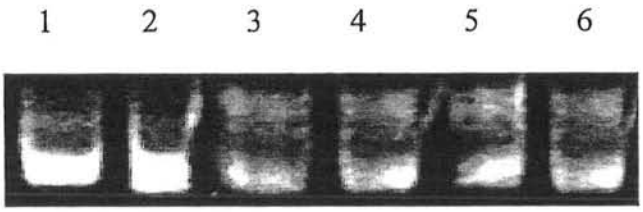

Family D

Lane 1.	IV-1	Affected	Lane 4.	III-1	Normal
Lane 2.	IV-6	Affected	Lane 5.	III-3	Normal
Lane 3.	III-4	Normal	Lane 6.	IV-4	Normal

Figure 3.43: Electropherogram of ethidium bromide stained 8% non-denaturing polyacrylamide gel for marker D9S1818 at 152.82 cM from MCPH7 candidate linkage interval on chromosome 9q34.3 of family D. The Roman numerals indicate the generation number of the individuals within a pedigree while Arabic numerals indicate their positions within generation.

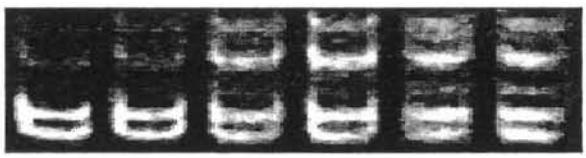

Family D

Lane 1.	IV-1	Affected	Lane 4.	III-1	Normal
Lane 2.	IV-6	Affected	Lane 5.	III-3	Normal
Lane 3.	III-4	Normal	Lane 6.	IV-4	Normal

Figure 3.44: Electropherogram of ethidium bromide stained 8% non-denaturing polyacrylamide gel for marker D9S1826 at 160.5 cM from MCPH7 candidate linkage interval on chromosome 9q34.3, of family D. The Roman numerals indicate the generation number of the individuals within a pedigree while Arabic numerals indicate their positions within generation.

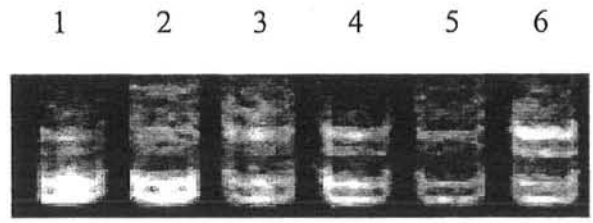

Family D

Lane 1.	IV-1	Affected	Lane 4.	III-1	Normal
Lane 2.	IV-6	Affected	Lane 5.	III-3	Normal
Lane 3.	III-4	Normal	Lane 6.	IV-4	Normal

Figure 3.45: Electropherogram of ethidium bromide stained 8% non-denaturing polyacrylamide gel for marker D9S158 at 163.08 cM from MCPH7 candidate linkage interval on chromosome 9q34.3 of family D. The Roman numerals indicate the generation number of the individuals within a pedigree while Arabic numerals indicate their positions within generation.

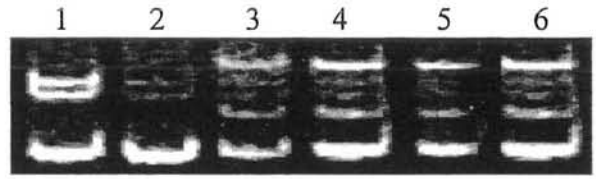

Family D

Lane 1.	IV-1	Affected	Lane 4.	III-1	Normal
Lane 2.	IV-6	Affected	Lane 5.	III-3	Normal
Lane 3.	III-4	Normal	Lane 6.	IV-4	Normal

Figure 3.46: Electropherogram of ethidium bromide stained 8% non-denaturing polyacrylamide gel for marker D9S905 at 165.24 cM from MCPH7 candidate linkage interval on chromosome 9q34.3 of family D. The Roman numerals indicate the generation number of the individuals within a pedigree while Arabic numerals indicate their positions within generation.

a

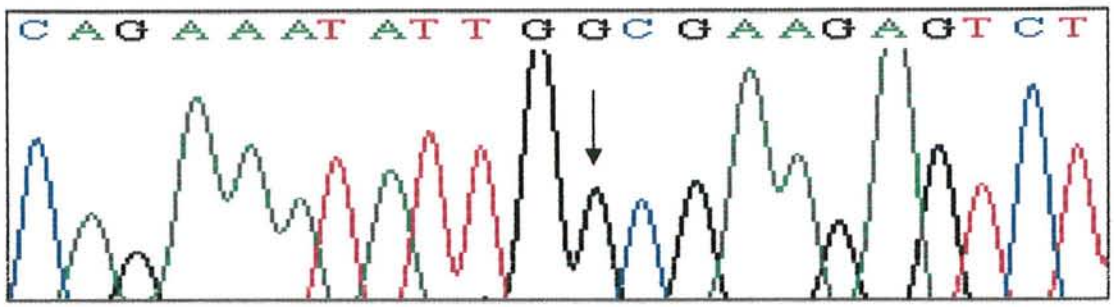

b

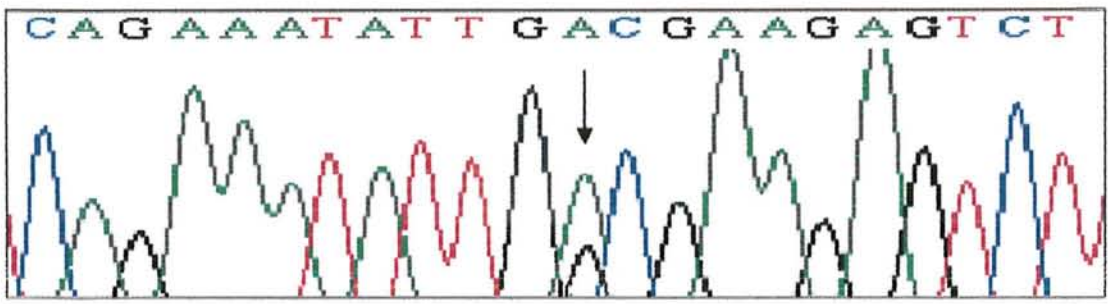

c

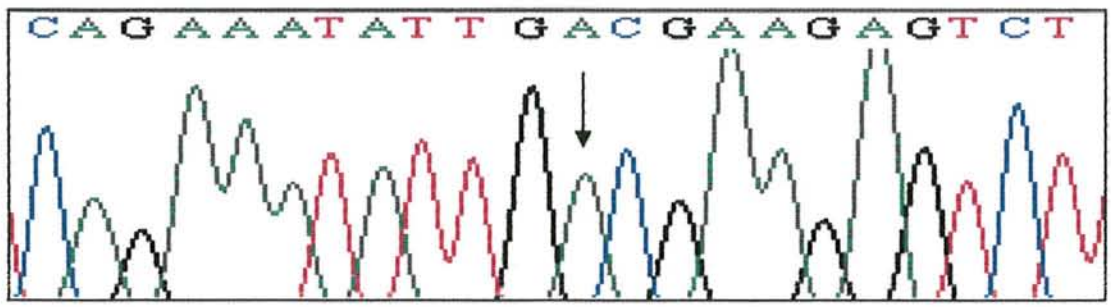

Figure 3.47: Sequencing chromatograms of exon 17 of *ASPM* gene in family C: (a) wild type sequence (b) heterozygous carrier (c) homozygous premature stop codon in exon 17 of *ASPM* gene in the affected individual.

DISCUSSION

DISCUSSION

Autosomal recessive primary microcephaly (MCPH) is a rare neurological disorder in which the head circumference of an affected individual is >3 SD below the population age and sex-related mean, and is also associated with nonprogressive mental retardation of variable degree (Woods *et al.*, 2005). In MCPH, MRI brain scans show that the whole brain is reduced in size and that it is the symmetrical reduction of the cerebral cortex, due to a decrease in the number of neurons that result in the small size (Bond *et al.*, 2002, 2003; Roberts *et al.*, 2002). This reduction in neurons can result from: (1) decreased proliferation of neuronal progenitors during symmetric mitosis; (2) decreased production of mature neurons by each neuronal progenitor during asymmetric mitosis; or (3) excessive apoptosis of neuronal progenitors or mature neurons (Mochida and Walsh, 2001). Regression or degeneration of established neural tissue can result in small brain size, but MCPH appears to arise through variation in the normal developmental process (Roberts *et al.*, 2002). The degree to which the cerebral cortex is reduced in MCPH varies. Mental retardation in the affected individuals ranges from mild to severe, but other neurological deficits are absent (Roberts *et al.*, 2002).

The MCPH is genetically heterogeneous with eight loci (MCPH1–MCPH8) mapped to date. Each locus was mapped in a multi-affected consanguineous family by autozygozity mapping using microsatellite markers spaced throughout the human genome: MCPH1 on chromosome 8p22-pter, MCPH2 on chromosome 19q13.1–13.2, MCPH3 on chromosome 9q34, MCPH4 on chromosome 15q, MCPH5 on chromosome 1q25–q32, MCPH6 on chromosome 13q12.2, and MCPH7 on chromosome 9q34.3. MCPH8 has already been discovered by Wood's group but not reported yet (personal communication). For these eight loci mutations in four genes including Microcephalin (Jackson *et al.*, 2002) at MCPH1, *CDK5RAP2* (Bond *et al.*, 2005; Hassan *et al.*, 2007) at MCPH3, *ASPM* (Bond *et al.*, 2002; Gul *et al.*,2006, 2007) at MCPH5 and *CENPJ* (Bond *et al.*, 2005; Gul *et al.*, 2006) at MCPH6 have been reported to cause clinically indistinguishable disorders.

In the present study, four highly consanguineous families (A, B, C and D), demonstrating primary microcephaly were ascertained from different regions of Pakistan. In all the families primary microcephaly was present by birth. The degree of

mental retardation varied from mild to moderate among affected individuals of these families. No crynosynotosis was observed in the affected individuals and also there were no environmental influence of the disease. Flat occiput and sharply sloping forehead was present in all affected individuals. Mode of inheritance was found to be compatible with an autosomal recessive trait.

To elucidate the gene defects in these families, linkage was performed by genotyping polymorphic microsatellite markers linked to seven known primary microcephaly loci. Genotyping analysis showed linkage of these families (A, B and C) to MCPH5 locus harboring *ASPM* gene. Therefore, *ASPM* gene was sequenced in affected and normal individuals of these three families.

In families A and B, the entire coding region and splice junctions of *ASPM* gene were screened in two affected and one normal individual of the families. Sequence analysis failed to detect pathogenic sequence variant suggesting that the mutation is probably present in the regulatory sequences of the gene. Family C, showed a previously characterized mutation 3978 G > A (Kumar *et al.*, 2004) in exon 17 of the *ASPM* gene (Figure 3.47). All the affected individuals were homozygous and the carriers were heterozygous for this mutation. The mutation resulted in changing codon TGG (Tryptophane) to TGA (stop codon), which in turn caused protein truncation and thus pathogenesis.

Genotyping analysis showed linkage of family D to MCPH7 locus harboring *INPP5E* gene. Therefore, *INPP5E* gene was sequenced in two affected and one normal individuals of the family. Sequence analysis of the entire coding region and splice junctions of *INPP5E* gene failed to detect pathogenic sequence variant suggesting that the mutation is probably present in the regulatory sequences of the gene. The protein encoded by *INPP5E* gene is an inositol 1, 4, 5-trisphosphate (InsP3) 5-phosphatase. Ins P3, 5-phosphatases hydrolyze Ins (1, 4, 5) P3, which mobilizes intracellular calcium and acts as a second messenger mediating cell responses to various stimulation. Studies of the mouse counterpart suggest that this protein may hydrolyze phosphatidylinositol 3, 4, 5-trisphosphate and phosphatidylinositol 3, 5-bisphosphate on the cytoplasm Golgi membrane and thereby regulate Golgi-vesicular trafficking.

In Pakistani population mutations in *ASPM* gene is the major cause of primary microcephaly. The gene *ASPM* (abnormal spindle-like microcephaly associated) is a

specific regulator of brain size, and its evolution in the lineage leading to *Homo sapiens* was driven by strong positive selection. *ASPM* is a major determinant of cerebral cortical size in MCPH5. It has an important role during mitosis in the normal spindle function in the early embryonic neuroblast. The *ASPM* gene contains 28 exons with a 10,434 bp long open reading frame (ORF) that codes for a 3477 amino-acid-long protein (Bond *et al.*, 2002). The ASPM protein is predicted to contain an amino terminal microtubuline-binding domain, a calponin homology domain, 74 isoleucine-glutamine (IQ) domains, and a C-terminal region (Bond *et al.*, 2002). The *ASPM* gene is expressed in fetal brain. The ASPM protein is conserved in human, mouse, Drosophila, and Caenorhabditis elegans with a consistent correlation of brain complexity and protein length, principally involving an increase in the number of encoded IQ domains (Bond *et al.*, 2002). It has been shown that most IQ motifs are organized into a higherorder trimer repeat (HOR) containing two 23-amino acid residue units and one 27-amino acid residue unit. The HOR structure is conserved in primate and mouse ASPM proteins, suggesting that such a structure is essential for the protein's function. The protein can bind calmodulin molecules with these IQ domains. Kouprina *et al.* (2005) have shown that calmodulin appears to regulate protein function by modulating its ability to bind to different targets either by altering the conformation of the protein or by influencing its subcellular locations. All the mutations known to date in *ASPM* gene are protein truncating whereas, only one mis-sense mutation is reported whose pathogenic consequence awaits further analysis (Gul *et al.,* 2006). The novel mutation found in the *ASPM* gene presented here also caused premature stop codon and hence protein truncation and in turn pathogenesis and hence asserts the earlier findings that the possible mechanism for disease pathogenesis in the *ASPM* gene is vivo a non-sense mutation resulting in protein truncation and destruction.

MCPH is hypothesized to be a primary disorder of neurogenic mitosis (Woods *et al.,* 2005). This assumption is strengthened by the presence of all the four known MCPH genes in the neuroepithelium of the developing brain (Jackson *et al.,* 2002; Bond *et al.,* 2003; Bond *et al.,* 2005) and also all of these have predictive roles in mitosis.

The discovery of primary microcephaly genes and their functions will help to understand neurodevelopmental processes. This may help our future generations to develop new therapeutics and diagonostic tools for its cure. Many other complex

disorders which may have overlapping gene pathways with MCPH may in turn be able to be better understood. This will only be possible when we have collected a very large genotypic database from different parts of the world, from different populations, cultures to identify all the loci and genes involved in the disease pathogenesis towards which the present study is a small but handy contribution.

REFERENCES

REFERENCES

Aicardi J (1998). Malformations of the central nervous system. In: Diseases of the nervous system in childhood. Mac keith Press, New York: pp 90-91

Alderton GK, Galbiati L, Griffith E, Surinya KH, Neitzel H, Jackson AP, Jeggo PA, O'Driscoll M (2006). Regulation of mitotic entry by microcephalin and its overlap with ATR signalling. Nat Cell Biol 8: 725-733

Avides do CM, Glover DM (1999). Abnormal spindle protein, Asp, and the integrity of mitotic centrosomal microtubule organizing centers. Science 283: 1733-1735

Avides do CM, Tavares A, Glover DM (2001). Polo kinase and Asp are needed to promote the mitotic organizing activity of centrosomes. Nat Cell Biol 4: 421-424

Baraitser P, Shieff C (1990). Cutaneomeningo-spinal angiomatosis: the syndrome of Cobb. A case report. Neuropediatrics 21: 160-161

Bennett RL, Steinhaus KA, Uhrich SB, O'Sullivan CK, Resta RG, Lochner-Doyle D, Markel DS, Vincent V, Hamanishi J (1995). Recommendations for standardized human pedigree nomenclature. Pedigree standardization task force of the national society of genetic counselors. Am J Hum Genet 56: 745-752

Bond J, Roberts E, Mochida GH, Hampshire DJ, Scott S, Askham JM, Springell K, Mahadevan M, Crow YJ, Markham AF, Walsh CA, Woods CG (2002). ASPM is a major determinant of cerebral cortical size. Nat Genet 32: 316-320

Bond J, Roberts E, Springell K, Lizarraga SB, Scott S, Higgins J, Hampshire DJ, Morrison EE, Leal GF, Silva EO, Costa SM, Baralle D, Raponi M, Karbani G, Rashid Y, Jafri H, Bennett C, Corry P, Walsh CA, Woods CG (2005). A centrosomal mechanism involving CDK5RAP2 and CENPJ controls brain size. Nat Genet 37: 353-355

Bond J, Scott S, Hampshire DJ, Springell K, Corry P, Abramowicz MJ, Mochida GH, Hennekam RC, Maher ER, Fryns JP, Alswaid A, Jafri H, Rashid Y, Mubaidin

A, Walsh CA, Roberts E, Woods CG (2003). Protein-truncating mutations in ASPM cause variable reduction in brain size. Am J Hum Genet 73: 1170-1177

Bond J, Woods CG (2006). Cytoskeletal genes regulating brain size. Curr Opin Cell Biol 18: 95-101

Bundey S (1997). Abnormal mental development. In: Emery and Rimoin's principles and practice of medical genetics, 3rd ed. Rimoin DL, Connor JM, Pyeritz RE (ed), Churchill Livingstone. New York 730: 140-146

Chaplet M, Rai R, Jackson-Bernitsas D, Li K, Lin SY (2006). A guardian of genome and an enemy of tumors. Cell Cycle 5: 2579-2583

Ching YP, Pang AS, Lam WH, Qi RZ, Wang JH (2002). Identification of a neuronal Cdk5 activator-binding protein as Cdk5 inhibitor. J Biol Chem 277: 15237-15240

Ching YP, Qi Z, Wang JH (2000). Cloning of three novel neuronal Cdk5 activator binding proteins. Gene 242: 285-294

Cho JH, Chang CJ, Chen CY, Tang TK (2006). Depletion of CPAP by RNAi disrupts centrosome integrity and induces multipolar spindles. Biochem Biophys Res Commun 339: 742-747

Cox J, Jackson AP, Bond J, Woods CG (2006). What primary microcephaly can tell us about brain growth. Trends Mol Med 12: 358-366

Craig R, Norbury C (1998). The novel murine calmodulin-binding protein Sha1 disrupts mitotic spindle replication checkpoint functions in fission yeast. J Cell Sci 111: 3609-3619

Dobyns WB (2002). Primary microcephaly: new approaches for an old disorder. Am J Med Genet 112: 315-317

Dolk H (1991). The predictive value of microcephaly during the first year of life for mental retardation at seven years. Dev Med Child Neurol 33: 974-983

Evans PD, Vallender EJ, Lahn BT (2006). Molecular evolution of the brain size regulator genes CDK5RAP2 and CENPJ. Gene 375: 75-79

Fish JL, Kosodo Y, Enard W, Pääbo S, Huttner WB (2006). Aspm specifically maintains symmetric proliferative divisions of neuroepithelial cells. Proc Natl Acad Sci USA 103: 10438-10443

Gul A, Hassan MJ, Hussain S, Raza SI, Chishti MS, Ahmad W (2006). A novel deletion mutation in CENPJ gene in a Pakistani family with autosomal recessive primary microcephaly. J Hum Genet 51: 760-764

Gul A, Hassan MJ, Mahmood S, Chen W, Rahmani S, Naseer MI, Dellefave L, Muhammad N, Rafiq MA, Ansar M, Chishti MS, Ali G, Siddique T, Ahmad W (2006). Genetic studies of autosomal recessive primary microcephaly in 33 Pakistani families: Novel sequence variants in ASPM gene. Neurogenetics 7: 105-110

Gul A, Tariq M, Khan MN, Hassan MJ, Ali G, Ahmad W (2007). Novel protein-truncating mutations in the ASPM gene in families with autosomal recessive primary microcephaly. J Neurogenet 21: 153-163

Hassan MJ, Khurshid M, Azeem Z, John P, Ali G, Chishti MS, Ahmad W (2007). Previously described sequence variant in CDK5RAP2 gene in a Pakistani family with autosomal recessive primary microcephaly. BMC Med Genet 8: 58

Horvath S, Zhang B, Carlson M, Lu KV, Zhu S, Felciano RM, Laurance MF, Zhao W, Qi S, Chen Z, Lee Y, Scheck AC, Liau LM, Wu H, Geschwind DH, Febbo PG, Kornblum HI, Cloughesy TF, Nelson SF, Mischel PS (2006). Analysis of oncogenic signaling networks in glioblastoma identifies ASPM as a molecular target. Proc Natl Acad Sci USA 103: 17402-17407

Hung LY, Tang CJ, Tang TK (2000). Protein 4.1 R-135 interacts with a novel centrosomal protein (CPAP) which is associated with the gamma-tubulin complex. Mol Cell Biol 20: 7813-7825

Huyton T, Bates PA, Zhang X, Sternberg MJ, Freemont PS (2000). The BRCA1 C-terminal domain: structure and function. Mutat Res 460: 319-332

Jackson AP, Eastwood H, Bell SM, Adu J, Toomes C, Carr IM, Roberts E, Hampshire DJ, Crow YJ, Mighell AJ, Karbani G, Jafri H, Rashid Y, Mueller RF, Markham AF, Woods CG (2002). Identification of microcephalin, a protein implicated in determining the size of the human brain. Am J Hum Genet 71: 136-142

Jackson AP, McHale DP, Campbell DA, Jafri H, Rashid Y, Mannan J, Karbani G, Corry P, Levene MI, Mueller RF, Markham AF, Lench NJ, Woods CG (1998). Primary autosomal recessive microcephaly (MCPH1) maps to chromosome 8p22-pter. Am J Hum Genet 63: 541-546

Jamieson CR, Fryns JP, Jacobs J, Matthijs G, Abramowicz MJ (2000). Primary autosomal recessive microcephaly: MCPH5 maps to 1q25-q32. Am J Hum Genet 67:1575-1577

Jamieson CR, Govaerts C, Abramowicz MJ (1999). Primary autosomal recessive microcephaly: homozygosity mapping of MCPH4 to chromosome 15. Am J Hum Genet 65: 1465-1469

Kouprina N, Pavlicek A, Collins NK, Nakano M, Noskov VN, Ohzeki J, Mochida GH, Risinger JI, Goldsmith P, Gunsior M, Solomon G, Gersch W, Kim JH, Barrett JC, Walsh CA, Jurka J, Masumoto H, Larionov V (2005). The microcephaly ASPM gene is expressed in proliferating tissues and encodes for a mitotic spindle protein. Hum Mol Genet 14: 2155-2165

Koyanagi M, Hijikata M, Watashi K, Masui O, Shimotohno K (2005). Centrosomal P4.1-associated protein is a new member of transcriptional coactivators for nuclear factor-kappaB. J Biol Chem 280: 12430-12437

Kumar A, Blanton SH, Babu M, Markandaya M, Girimaji SC (2004). Genetic analysis of primary microcephaly in Indian families: novel ASPM mutations. Clin Genet 66: 341-348

Leal GF, Roberts E, Silva EO, Costa SM, Hampshire DJ, Woods CG (2003). A novel locus for autosomal recessive primary microcephaly (MCPH6) maps to 13q12.2. J Med Genet 40: 540-542

Leidel S, Gonczy P (2005). Centrosome duplication and nematodes: recent insights from an old relationship. Dev Cell 9: 317-325

Lin SY, Rai R, Li K, Xu ZX, Elledge SJ (2005). BRIT1/MCPH1 is a DNA damage responsive protein that regulates the Brca1-Chk1 pathway, implicating checkpoint dysfunction in microcephaly. Proc Natl Acad Sci USA 102: 15105-15109

Mochida GH, Walsh CA (2001). Molecular genetics of human microcephaly. Curr Opin Neurol 14: 151-156

Moynihan L, Jackson AP, Roberts E, Karbani G, Lewis I, Corry P, Turner G, Mueller RF, Lench NJ, Woods CG (2000). A third novel locus for primary autosomal recessive microcephaly maps to chromosome 9q34. Am J Hum Genet 66: 724-727

Neitzel H, Neumann LM, Schindler D, Wirges A, Tonnies H, Trimborn M, Krebsova A, Richter R, Sperling K (2002). Premature chromosome condensation in humans associated with microcephaly and mental retardation: a novel autosomal recessive condition. Am J Hum Genet 70: 1015-1022

Opitz JM, Holt MC (1990). Microcephaly: general considerations and aids to nosology. J Craniofac Genet Dev Biol 10: 175-204

Pattison L, Crow YJ, Deeble VJ, Jackson AP, Jafri H, Rashid Y, Roberts E, Woods CG (2000). A fifth locus for primary autosomal recessive microcephaly maps to chromosome 1q31. Am J Hum Genet 67: 1578-1580

Peng B, Sutherland KD, Sum EY, Olayioye M, Wittlin S, Tang TK, Lindeman GJ, Visvader JE (2002). CPAP is a novel stat5-interacting cofactor that augments stat5-mediated transcriptional activity. Mol Endocrinol 16: 2019-2033

Qazi QH, Reed TE (1973). A problem in diagnosis of primary versus secondary microcephaly. Clin Genet 4: 46-52

Rajab A, Mochida GH, Hill A, Ganesh V, Bodell A, Riaz A, Grant PE, Shugart YY, Walsh CA (2003). A novel form of pontocerebellar hypoplasia maps to chromosome 7q11-21. Neurology 60: 1664

Roberts E, Hampshire DJ, Pattison L, Springell K, Jafri H, Corry P, Mannon J, Rashid Y, Crow Y, Bond J, Woods CG (2002). Autosomal recessive primary microcephaly: an analysis of locus heterogeneity and phenotypic variation. J Med Genet 39: 718-721

Roberts E, Jackson AP, Carradice AC, Deeble VJ, Mannan J, Rashid Y, Jafri H, McHale DP, Markham AF, Lench NJ, Woods CG (1999). The second locus for autosomal recessive primary microcephaly (MCPH2) maps to chromosome 19q13.1-13.2. Eur J Hum Genet 7: 815-820

Rosenberg MJ, Agarwala R, Bouffard G, Davis J, Fiermonte G, Hilliard MS, Koch T, Kalikin LM, Makalowska I, Morton DH, Petty EM, Weber JL, Palmieri F, Kelley RI, Schaffer AA, Biesecker LG (2002). Mutant deoxynucleotide carrier is associated with congenital microcephaly. Nat Genet 32: 175-179

Ross JJ, Frias JL (1977). Microcephaly. In: Congenital malformations of the brain and skull, Vinken PJ, Bruyn GW (ed). Biomedical Press, Holland: pp 507-524

Shahbazian MD, Zoghbi HY (2002). Rett syndrome and MeCP2: linking epigenetics and neuronal function. Am J Hum Genet 71: 1259-1272

Shen J, Eyaid W, Mochida GH, Al-Moayyad F, Bodell A, Woods CG, Walsh CA (2005). ASPM mutations identified in patients with primary microcephaly and seizures. J Med Genet 42: 725-729

Tang BL (2006). Molecular genetic determinants of human brain size. Biochem Biophys Res Commun 345: 911-916

Teebi AS, Al-Awadi SA, White AG (1987). Autosomal recessive nonsyndromal microcephaly with normal intelligence. Am J Med Genet 26: 355-359

Tolmie JL, McNay M, Stephenson JB, Doyle D, Connor JM (1987). Microcephaly: genetic counselling and antenatal diagnosis after the birth of an affected child. Am J Med Genet 27: 583-594

Trimborn M, Bell SM, Felix C, Rashid Y, Jafri H, Griffiths PD, Neumann LM, Krebs A, Reis A, Sperling K, Neitzel H, Jackson AP (2004). Mutations in microcephalin cause aberrant regulation of chromosome condensation. Am J Hum Genet 75: 261-266

Trimborn M, Richter R, Sternberg N, Gavvovidis I, Schindler D, Jackson AP, Prott EC, Sperling K, Gillessen-Kaesbach G, Neitzel H (2005). The first missense alteration in the MCPH1 gene causes autosomal recessive microcephaly with an extremely mild cellular and clinical phenotype. Hum Mutat 26: 496

Tunçbilek E (2001). Clinical outcomes of consanguineous marriages in Turkey. Turk J Pediatr 43: 277-279

Woods CG, Bond J, Enard W (2005). Autosomal recessive primary microcephaly (MCPH): a review of clinical, molecular, and evolutionary findings. Am J Hum Genet 76: 717-728

Electronic Database Information

- Ensemble Genome Browser

  URL: http//www.ensemble.org/index.html

- Genome Database Homepage.

  URL: http//www.gdb.org

- Human Gene Mutation Database

  URL: http//www.hgmd.org

- Marshfield Medical Center.

  URL: http//www.marshmed.org.gov/genetics

- Online Mendelian Inheritance in Man

  URL: http://www.ncbi.nlm.nih.gov

- UCSC Genome Bioinformatics

  URL: http//www.genome.ucsc.edu

Electronic Database Information

- Ensemble Genome Browser

  URL: http//www.ensemble.org/index.html

- Genome Database Homepage.

  URL: http//www.gdb.org

- Human Gene Mutation Database

  URL: http//www.hgmd.org

- Marshfield Medical Center.

  URL: http//www.marshmed.org.gov/genetics

- Online Mendelian Inheritance in Man

  URL: http://www.ncbi.nlm.nih.gov

- UCSC Genome Bioinformatics

  URL: http//www.genome.ucsc.edu